Approximate Methods for the Simulation of
Groundwater Contamination Processes
by
Hillel Rubin*
Kansas Geological Survey Open-File Report 94-8

Table of Contents 1

*On leave from the Department of Civil Engineering, Technion—Israel Institute of Technology, Haifa 32000, Israel.

List of Figures

Fig. 11 Steady state values of δ according to all approximations ($a = 0.5$, $a_L = 5$, $n = 3$).

Fig. 12 Comparison between values of δ according to eq. (22) and the TSBL method [eqs. (39, (41)] ($a = 0.5$, $n = 3$).

Fig. 13 Build-up of the contaminant concentration profiles in space and time as obtained by use of eq. (15) ($q_R = 0.1$, $a = 0.5$, $a_L = 5$).

(a) $t = 25$; (b) $t = 50$; (c) $t = 75$; (d) $t = 100$

Fig 14 Build-up of the ROI in which $C \geq 0.01$, as obtained by use of eq. (15) ($q_R = 0.1$, $a = 0.5$, $a_L = 5$).

Fig. 15 Development of C_b in time and along the free surface of the aquifer according to eq. (15) ($q_R = 0.1$, $a = 0.5$, $a_L = 5$).

Fig. 16 Steady state profiles of C in various cross sections according to eq. (26) ($q_R = 0.1$, $a = 0.5$).

(a) $x = 10, 20, 30, 40, 50$

(b) comparison with eq. (19) ($a_L = 5$).

$x = 20, 50$

Fig. 17 Steady state C/C_b profiles versus y/δ_0 in various cross sections.

(a) $q_R = 0.001$; $a = 0.1$

(b) $q_R = 0.01$; $a = 0.1$

(c) $q_R = 0.01$; $a = 1$

(d) $q_R = 0.1$; $a = 0.5$

Fig. 18 Comparison between different power series expansions and C/C_b profiles at $x = 50$.

(a) $q_R = 0.001$; $a = 0.1$, $q_R/a = 0.01$

(b) $q_R = 0.01$; $a = 0.1$, $q_R/a = 0.1$

(c) $q_R = 0.01$; $a = 1$, $q_R/a = 0.01$

(d) $q_R = 0.1$; $a = 0.5$, $q_R/a = 0.2$

Fig. 19 Comparison between steady state values of δ and δ_0 obtained by TSBL approach and values of δ obtained by eq. (26).

(a) $q_R = 0.1$; $a = 0.5$, $n = 4$; ($q_R/a = 0.2$)

(b) $q_R = 0.001$; $a = 0.1$, $n = 3$; ($q_R/a = 0.01$)

Fig. 20 Comparison between steady state values of C_b predicted by the TSBL method and values obtained by use of eq. (26).

Curves A—$q_R = 0.1$; $a = 0.5$, $n = 4$

Curves B—$q_R = 0.001$; $a = 0.1$, $n = 3$ (values are multiplied by 10)

Fig. 21 Development of the ROI according to the TSBL method and the numerical scheme of eq. (22) ($q_R = 0.1$; $a = 0.5$, $n = 4$)

Abstract

This report presents improvements in the classical boundary layer (CBL) approximation method to obtain simple but robust initial characterizations of aquifer contamination processes. Contaminants are considered to penetrate into the groundwater through the free surface of the aquifer. By specifying concentration values for the boundary of the "region of interest" (ROI) simulated as a boundary layer (BL), the CBL method is improved to obtain the "top specified boundary layer" (TSBL) method. By use of the TSBL the ability to predict the development of concentration profiles over both space and time is greatly improved. The TSBL approach developed in this study can be useful for cases in which the contaminant concentration is prescribed at the aquifer's free surface as well as for cases in which the contaminant mass flux is prescribed at the surface.

In the framework of this study the usage of a hierarchy of approximate methods, leading to the TSBL approach, is presented and evaluated. It is considered that such a presentation provides all information needed for the adoption of the TSBL application in various cases and phenomena of groundwater contamination.

Notation

a	dimensionless transverse dispersivity
a_L	dimensionless longitudinal dispersivity
$a_0, a_1 a_2...$	power series coefficients defined in eq. (32)
BL	boundary layer
C	normalized contaminant concentration
C_b	normalized concentration at the aquifer's surface
C_T	normalized concentration at the top of the BL
C_1	normalized concentration at y_1
C_2	normalized concentration at y_2
C^*	contaminant concentration [ML^{-3}]
C_0	concentration of reference[ML^{-3}]
CBL	classical boundary layer
d	represents δ in figures
d_0	represents δ_0 in figures
$\tilde{D}$	dispersion tensor [L^2T^{-1}]
D_x	longitudinal dispersion coefficient [L^2T^{-1}]
D_y	transverse dispersion coefficient [L^2T^{-1}]
g	gravitational acceleration
k	permeability [L^2]
l_0	length scale[L]
L	power series
m	number of time step
n	power coefficient
(n)	number of iteration
p	pressure [$ML^{-1}T^{-2}$]
q	specific discharge of the aquifer [LT^{-1}]

q_m	mass flux of the penetrating contaminant into the aquifer [$ML^{-2}T^{-1}$]
q_R	relative penetrating mass flux
r	number of the nodal point in the longitudinal direction
ROI	region of interest
s	number of the nodal point in the vertical direction
t	dimensionless time
t^*	time [T]
t_0	time scale [T]
TSBL	top specified boundary layer
u	a step function defined in eq. (42)
V	interstitial flow velocity [LT^{-1}]
x	dimensionless longitudinal coordinate
x_{max}	length of the domain
x_b	starting point for the development of the ROI
x*	longitudinal coordinate [L]
y	dimensionless vertical coordinate
y_1	value of y at which $C = C_1$
y_2	value of y at which $C = C_2$
y*	vertical coordinate [L]
$\alpha_0, \alpha_1, \alpha_2, \alpha_3...$	coefficients defined in eq. (20)
δ	dimensionless thickness of the ROI
δ_0	dimensionless ordinate of practically zero contaminant concentration
Δt	time step
Δx	longitudinal interval
Δy	vertical interval
θ	dimensionless coordinate defined in eq. (51)
η	dimensionless coordinate of the boundary layer

η_T	value of y at $y = \delta$
μ	fluid viscosity [$ML^{-1}T^{-1}$]
ρ	fluid density [ML^{-3}]
ϕ	porosity
ω	over-relaxation coefficient

Introduction

The boundary layer (BL) approximation as an integral method for the solution of partial differential equations dates back to von-Karman and Pohlhausen, who applied this method to phenomena of fluid flow (Schlichling, 1968). Since then the BL approximation has been useful in a variety of topics associated with fluid flows, heat transfer and mass transfer (Ozisik, 1980).

The application of the BL approximation to the calculation of transport phenomena in groundwater was demonstrated in various studies. Wooding (1963; 1964; 1971) developed a BL theory for plane vertical as well as horizontal flows in porous media, and showed that for large Rayleigh or Peclet numbers the diffusion zone between two miscible fluids behaves like a BL. Then diffusion-advection of arbitrary tracers can be solved into two parts corresponding to two physical regions—the outer region, where diffusion is negligible and the inner region in which diffusion is important but BL approximations are valid. By matching the inner and outer expansions as explained by Van Dyke (1964) and Cole (1968) a complete description of the tracer distribution in the domain is developed.

Dagan (1971) formulated the equation of diffusion-advection for a tracer in a domain subject to steady-state conditions by applying a coordinate system based on the potential and stream functions (Bachmat and Bear, 1964). Then by applying singular perturbations as suggested by Wooding (1963, 1964) he analyzed the migration of the tracer front. In a later study Eldor and Dagan (1972) extended the analysis to include radioactive decay and absorption.

Gelhar and Collins (1971) applied a BL approximation to develop general solutions for one dimensional diffusion-advection of neutrally buoyant tracers in porous media.

Hunt extended the approach outlined by Wooding and Dagan for general cases concerning the migration of neutrally buoyant tracers in heterogeneous aquifers.

Various studies (e.g. Rubin and Pinder, 1979; Rubin, 1983; Rubin and Pistiner, 1986; McElwee and Kemblowski, 1990) employed the BL approximation to analyze mineralization processes in groundwater.

All studies reviewed in preceding paragraphs apply the classical BL, namely CBL, approximation. According to the CBL approach the diffusion-advection equation is solved for certain classes of problems in which the transported quantity is prescribed at some boundary locations. The contaminant is assumed to be practically distributed at a small region called BL. This region is extended between the boundary of the prescribed quantity and the top of the BL, at which the quantity concentration practically vanishes.

The objective of the present study is to apply a hierarchy of approximation methods to the calculation and analysis of contamination of groundwater by contaminant penetrating through the free surface of the aquifer. We intend to pay special attention to the CBL approach, improve its performance and its scope of uses. Our ultimate goal is to develop simple but robust approach to the initial characterization of aquifer contamination processes.

The Conceptual Model and Basic Formulation

We refer to a simplified conceptual model of an aquifer subject to contamination as shown in fig. 1(a). The aquifer is unconfined, and saturated thickness is great enough so that the Dupuit approximation can be useful. Flow direction and streamlines are almost horizontal. The longitudinal x^* axis represents the surface through which contaminants are introduced into the aquifer. The y^* axis is vertical in the downward direction.

Flow conditions and contaminant transport in the domain of fig. 1(a) are governed by the following differential equations:

$$\vec{q} = -\frac{k}{\mu}(\nabla p - \rho \vec{g}) \tag{1}$$

$$\frac{\partial C^*}{\partial t^*} + \vec{V} \cdot \nabla C^* = \nabla \cdot \left(\tilde{D} \cdot \nabla C^*\right) \tag{2}$$

where, q is the specific discharge; k is the permeability; μ is the fluid viscosity; p is the pressure; ρ is the fluid density; g is the gravitational acceleration; C^* is the contaminant concentration; V is the interstitial flow velocity; $\tilde{D}$ is the dispersion tensor; and t^* is the time.

The system of partial differential eqs. (1) and (2) can be solved by various types of numerical procedures. However, the Dupuit approximation is usually employed for the solution of eq. (1). In the particular case of the domain shown in fig. 1(a), this approximation yields a uniform horizontal flow velocity, provided that the permeability is uniform. Then eq. (2) is represented as

$$\frac{\partial C^*}{\partial t^*} + V\frac{\partial C^*}{\partial x^*} = D_x\frac{\partial^2 C^*}{\partial x^{*2}} + D_y\frac{\partial^2 C^*}{\partial y^{*2}} \tag{3}$$

where x^* and y^* are the longitudinal and vertical coordinates, respectively; D_x and D_y are the longitudinal and transverse dispersion coefficients, respectively.

As the domain is homogeneous and isotropic we may refer to the following characteristics of the domain

$$l_0,\ t_0 = l_0 / V,\ C_0 \tag{4}$$

where l_0 is an adopted unit length along the surface $y^* = 0$; t_0 is the time corresponding to l_0 for the velocity V; C_0 is a concentration of reference. The value of C_0 should somehow be connected with prescribed boundary values or risk values of the contaminant concentration.

The characteristics of eq. (4) are used to nondimensionalize the variables of eq. (3) as

$$x = x^* / l_0;\ y = y^* / l_0;\ t = t^* / t_0;\ C = C^* / C_0 \tag{5}$$

Introducing these terms into eq. (3) we obtain

$$\frac{\partial C}{\partial t} + \frac{\partial C}{\partial x} = a_L\frac{\partial^2 C}{\partial x^2} + a\frac{\partial^2 C}{\partial y^2} \tag{6}$$

where a_L and a are the dimensionless longitudinal and transverse disperisivities which are defined as

$$a_L = D_x / (l_0 V);\ a = D_y / (l_0 V) \tag{7}$$

The following sections of this report are devoted to the development of solutions to eq. (6) subject to initial and boundary conditions relevant to cases of groundwater contamination in aquifers that can approximately be described by the conceptual model shown in fig. 1(a).

If at the boundary $y = 0$ the value of the contaminant concentration is prescribed, then it seems reasonable to adopt

$$C_0 = C^*(x^*, 0, t^*) \tag{8}$$

namely, contaminant concentrations are normalized with regard to the concentration at the x^* axis. Under such conditions eq. (6) is subject to the following initial and boundary conditions.

$$\begin{aligned} &C = C(x,y,t) \quad x,y,t \geq 0 \\ &C(x,y,0) = 0 \quad \textit{except for } C(x,0,0) = 1.0 \\ &C(x,0,t) = 1 \\ &C(0,y,t) = 0 \\ &C(x,\infty,t) = 0 \\ &\frac{\partial C}{\partial x} \to 0 \ \textit{at} \ x \to \infty \end{aligned} \tag{9}$$

In fig. 1(b) the dimensionless domain and quantities are shown for the prescribed contaminant concentration at $y = 0$. Some of these quantities will be defined in following sections of this report.

If at the boundary $y = 0$, is prescribed the contaminant mass flux which penetrates into the groundwater, then

$$\phi D_y \frac{\partial C^*}{\partial y^*} = -q_m \ \textit{at} \ y^* = 0 \tag{10}$$

where, q_m is the contaminant mass flux penetrating into the domain through the x^* axis; and ϕ is the porosity of the porous medium.

By introducing the normalized quantities of eqs. (5) and (7) into eq. (10) we obtain

$$a\frac{\partial C}{\partial y} = -q_R \ \textit{at} \ y = 0 \tag{11}$$

where, q_R is the normalized flux of the penetrating contaminant

$$q_R = \frac{q_m}{qC_0} \tag{12}$$

where, q is the specific discharge of the aquifer flow.

The following initial and boundary conditions are applicable when the contaminant mass flux is prescribed at $y = 0$.

$$\begin{aligned} &C = C(x,y,t) \quad x,y,t \geq 0 \\ &C(x,y,0) = 0 \end{aligned}$$

$$\frac{\partial C}{\partial y} = -\frac{q_R}{a} \quad at \quad y = 0$$

$$C(0, y, t) = 0$$

$$C(x, \infty, t) = 0$$

$$\frac{\partial C}{\partial x} \to 0 \quad at \quad x \to \infty \tag{13}$$

In fig. 1(c) the dimensionless domain and quantities are shown for the prescribed contaminant flux penetrating into groundwater at $y = 0$.

Direct Solution of the Contaminant Transport Equation

Equation (6) can be solved by various types of numerical procedures. In the framework of the present study, we use finite difference schemes whose performance can easily be analyzed and evaluated.

The initial and boundary conditions represented by eqs. (9) and (13) indicate that when the numerical simulation starts, all terms of eq. (6) have vanishing values. As long as both terms of the right hand side of eq. (6) are very small, that equation is approximately a first order hyperbolic equation in the x, t plane. If the second term of the left-hand side is small then eq. (6) is approximately a parabolic equation in the x, t and y, t planes. If steady state conditions are established in the domain, then the first term of eq. (6) vanished. Under such conditions eq. (6) is converted to an elliptic partial differential equation. However, if in steady state the first-right-hand-side term is much smaller than the last term of eq. (6) then this equation is converted to a parabolic equation in the x, y plane.

The preceding paragraph indicates that some prior studies of the nature of eq. (6) and its relationship to the hydrologic characteristics of the aquifer under consideration may enable the use of simplified schemes for the solution of eq. (6). However, in the first stage we develop a stable numerical scheme for the solution of eq. (6).

Because of the possible parabolic feature of eq. (6), it is reasonable to adopt a forward finite difference approximation with regard to Δt.

In order to obtain a stable hyperbolic system we may adopt central or backward stable approximation scheme with regard to the second left-hand-side term of eq. (6). The central-difference approximation has a smaller truncation error than the backward schemes. The combination of either central or backward space difference with the forward time difference is subject to a certain amount of numerical dispersion.

Explicit schemes can be adopted provided that the following condition is satisfied (e.g. Lapidus and Pinder, 1982).

$$\frac{\Delta t}{\Delta x} \leq 1 \tag{14}$$

Implicit schemes are not subject to such a limitation. Choice of the central space difference for the second left-hand-side term if eq. (6) leads to an implicit scheme. Choice of backward space difference for that term may lead to explicit schemes, from which we choose to apply the following one

$$\begin{aligned} C_{r,s}^{m+1}\left(1+\frac{\Delta t}{\Delta x}\right) &= C_{r,s}^{m}+\frac{\Delta t}{\Delta x}C_{r-1,s}^{m+1} \\ &+\frac{a_L\Delta t}{(\Delta x)^2}\left(C_{r+1,s}^{m}-2C_{r,s}^{m}+C_{r-1,s}^{m}\right)+\frac{a\Delta t}{(\Delta y)^2}\left(C_{r,s+1}^{m}-2C_{r,s}^{m}+C_{r,s-1}^{m}\right) \end{aligned} \tag{15}$$

where, Δx, Δy and Δt are intervals of x, y and t, respectively; r is the number of the longitudinal node; s is the number of the vertical node, m is the number of the time step.

By the employment of the procedure of von-Neumann (e.g. Lapidus an Pinder, 1982) the following stability criteria for the scheme of eq. (15) are obtained.

$$\begin{aligned} \frac{2a_L\Delta t}{(\Delta x)^2}+\frac{2a\Delta t}{(\Delta y)^2} &\leq 1+\frac{\Delta t}{\Delta x} \\ \frac{2a\Delta t}{(\Delta y)^2} &\leq 1 \end{aligned} \tag{16}$$

When steady state conditions are established in the domain, we may consider

$$C_{r,s}^{m+1} = C_{r,s}^{m} = C_{r,s} \tag{17}$$

By introducing eq. (17) into eq. (15) we obtain

$$C_{r,s}\left[1+\frac{2a_L}{\Delta x}+\frac{2a\Delta x}{(\Delta y)^2}\right] = C_{r-1,s}\left[1+\frac{a_L}{\Delta x}\right]+\frac{a_L}{\Delta x}C_{r+1,s}+\frac{a\Delta x}{(\Delta y)^2}\left(C_{r,s-1}+C_{r,s+1}\right) \tag{18}$$

Basically, as stated before, when steady state conditions are established, eq. (6) becomes an elliptic partial differential equation in the x, y plane. According to eq. (18) each nodal point (r, s) in the domain is associated with five unknown values of C in (r, s) and surrounding nodal points. The constant coefficient multiplying $C_{r,s}$ is the dominant factor in all equations referring to all nodal points of the domain. Therefore, the solution of the set of linear equations represented by eq. (18) can efficiently be solved by the successive overrelaxation (SOR) method. The iterative procedure is given by

$$C_{r,s}^{(n+1)} = (1-\omega)C_{r,s}^{(n)} + \omega\left[\alpha_1 C_{r-1,s}^{(n+1)} + \alpha_2 C_{r+1,s}^{(n)} + \alpha_3\left(C_{r,s-1}^{(n+1)} + C_{r,s+1}^{(n)}\right)\right] \tag{19}$$

where

$$\alpha_0 = 1 + 2\frac{a_L}{\Delta x} + \frac{2a\Delta x}{(\Delta y)^2};\ \alpha_1 = \left(1 + \frac{a_L}{\Delta x}\right)/\alpha_0$$

$$\alpha_2 = \left(\frac{a_L}{\Delta x}\right)/\alpha_0;\ \alpha_3 = \left[\frac{a\Delta x}{(\Delta y)^2}\right]/\alpha_0 \tag{20}$$

In eq. (19), (n) is the number of the iteration; ω is the overrelaxation coefficient.

Neglect of Longitudinal Dispersion

Due to the specific features of the domain shown in fig. 1 contaminants are transferred in the x direction mainly due to the advection mechanism. On the other hand effective diffusion is the major mechanism leading to contaminant transfer in the y direction. Some preliminary tests exemplified in the following section "Calculations and Results" show that the contaminant distribution in the domain is almost unaffected by the variation of a_L.

Therefore, we may consider the complete neglect of the first right-hand-side term of eq. (6). A quantitative evaluation of such an approach is given in the "Calculations and Results" section.

The complete neglect of longitudinal dispersion modifies eq. (6) to

$$\frac{\partial C}{\partial t} + \frac{\partial C}{\partial x} = a\frac{\partial^2 C}{\partial y^2} \tag{21}$$

If the right hand side term of eq. (21) is very small, then eq. (21) is a hyperbolic first order equation; otherwise it can be a parabolic type equation in the y, t or x, y planes. We apply

considerations similar to those presented in the previous section and adopt the following explicit scheme for the solution of eq. (21)

$$C_{r,s}^{m+1}\left(1+\frac{\Delta t}{\Delta x}\right)=C_{r,s}^{m}+\frac{\Delta t}{\Delta x}C_{r-1,s}^{m+1}+\frac{a\Delta t}{(\Delta y)^2}\left(C_{r,s+1}^{m}-2C_{r,s}^{m}+C_{r,s-1}^{m}\right) \tag{22}$$

By the employment of the von-Neumann procedure (e.g. Lapidus and Pinder, 1982), the following stability criterion of the numerical scheme, given by eq. (22), is obtained.

$$\frac{2a\Delta t}{(\Delta y)^2}\leq 1 \tag{23}$$

It should be noted that eq. (21) can be converted into a parabolic equation in the x, y plane by the employment of the Laplace transform. However, the solution of the equation in the Laplace transform plane and subsequent return to the x, y, t domain for implementation of the various possible boundary conditions at $y = 0$ is complicated.

When steady state conditions are established in the domain eq. (21) collapses to

$$\frac{\partial C}{\partial x}=a\frac{\partial^2 C}{\partial y^2} \tag{24}$$

This equation is analogous to the typical diffusion or heat conduction equation in a one dimensional domain. Equation (24) is a parabolic partial differential equation in the x, y domain. If we refer to the contamination case in which the contaminant concentration is prescribed at $y = 0$, we obtain by the analogy to heat conduction (Carslaw and Jaeger, 1959).

$$C=erfc\left[y/(4ax)^{0.5}\right] \tag{25}$$

where, *erfc* is the complementary error function. If the constant flux of the penetrating contaminant is prescribed at $y = 0$, then we obtain (Carslaw and Jaeger, 1959)

$$C=\frac{q_R}{a}\left[2\sqrt{\frac{ax}{\pi}}\exp\left(\frac{-y^2}{4ax}\right)-y\ erfc\left(\frac{y}{2\sqrt{ax}}\right)\right] \tag{26}$$

The Top Specified Boundary Layer (TSBL) Approach

The proof of the applicability of eq. (21), as shown in the "Calculations and Results" section, for the calculation of contaminant transport in the domain of fig. 1 encourages the use of the boundary layer (BL) approximation to simulate contaminant transport. However, some

changes and improvements are done in the framework of this study in order to increase the reliability of the classical boundary layer (CBL) and make it applicable to a larger scope of environmental problems.

To apply the BL approach we define a "region of interest" (ROI), in which the contaminant concentration is higher than a certain acceptable level. The thickness of that region is δ where

$$\delta = \delta(x,t) \tag{27}$$

From practical view point we assume that contaminant concentration vanishes where the contaminant concentration is lower by at least an order of magnitude than the acceptable level. The contaminant concentration goes to zero at δ_0 where

$$\delta_0 = \delta_0(x,t);\ \delta_0 > \delta \tag{28}$$

We assume that in the contaminated region

$$C = C_b L(\eta);\ \eta = y/\delta_0 \tag{29}$$

where C_b is the contaminant concentration at $y = 0$. The ROI is extended between $y = 0$ and $y = \delta$. The ordinate $y = \delta$ is termed as the top of the BL which simulates the boundary of the ROI. At that location

$$y = \delta;\ \eta = \eta_T = \delta/\delta_0;\ C = C_T = C_b L(\eta_T) \tag{30}$$

namely contaminant concentration is specified as C_T at the top of the boundary layer. Therefore, the method is termed as "top specified boundary layer" (TSBL).

We integrate eq. (21) along the vertical y coordinate between $y = 0$ and $y = \delta_0$ and use Leibniz's theorem to obtain

$$\frac{\partial}{\partial t}\left(\int_0^{\delta_0} C dy\right) + \frac{\partial}{\partial x}\left(\int_0^{\delta_0} C dy\right) = -a\left[\frac{\partial C}{\partial y}\right]_{y=0} \tag{31}$$

We consider that the function L(η) given in eq. (29) can be represented by a power series as

$$L(\eta) = a_0 + a_1\eta + a_2\eta^2 + \ldots \tag{32}$$

where a_0, a_1. . . are constant coefficients.

It should be noted that the number of terms incorporated in L(η) is determined only by the desired fit of eq. (29) to measured values of C/C_b.

We consider the following boundary conditions for the determination of the coefficients of the power series L(η)

$$L(0)=1; \quad L(1)=0;$$
$$\frac{d^n L(1)}{d\eta^n}=0 \qquad n=1,2,... \tag{33}$$

Equations (32) and (33) imply

$$L(\eta)=(1-\eta)^n \tag{34}$$

Equation (34) indicates that from a more general view point than that given by eq. (32), it is possible to adopt values of n that are not integers.

Introducing eq. (20) into eq. (31), we obtain

$$\frac{\partial}{\partial t}(\delta_0 C_b)+\frac{\partial}{\partial x}(\delta_0 C_b)=-\frac{aC_b L'(0)}{\delta_0 \int_0^1 L d\eta} \tag{35}$$

The following quantities are obtained by using eq. (34)

$$L'(0)=-n; \quad \int_0^1 L d\eta = 1/(n+1) \tag{36}$$

In following paragraphs we discuss first the prescribed contaminant concentration at $y=0$, followed by the prescribed contaminant flux at $y=0$.

If constant contaminant concentration is prescribed at $y=0$, we consider

$$C_b=1 \tag{37}$$

Introducing eqs. (36) and (37) into eq. (35) we obtain

$$\frac{\partial}{\partial t}(\delta_0^2)+\frac{\partial}{\partial x}(\delta_0^2)=2an(n+1) \tag{38}$$

Equation (38) is subject to the following initial and boundary conditions

$$\delta_0=\delta_0(x,t)$$
$$\delta_0(x,0)=0$$
$$\delta_0(0,t)=0 \tag{40}$$

Equation (38), subject to the initial and boundary conditions, can easily be solved by the Laplace transform method to obtain

$$\delta_0^2 = 2an(n+1)[t-(t-x)u(t-x)] \tag{41}$$

where

$$u(t-x) = \begin{cases} 1 & t > x \\ 0 & t < x \end{cases} \tag{42}$$

According to eq. (41) steady state conditions are established in the domain when $t = x_{max}$, where x_{max} is the length of the domain.

Equations (39) and (41) provide analytical expressions for δ_0 and δ in space and time. These equations in conjunction with eqs. (29) and (34) provide the information concerning the contaminant distribution in the ROI.

If constant contaminant mass flux is prescribed at $y = 0$, we employ eqs. (11), (29) and (36) to obtain

$$C_b = -\frac{q_R \delta_0}{aL'(0)} = \frac{q_R \delta_0}{an} \tag{43}$$

Introducing eqs. (36) and (40) into eq. (35), we obtain

$$\frac{\partial}{\partial t}\left(\delta_0^2\right) + \frac{\partial}{\partial x}\left(\delta_0^2\right) = an(n+1) \tag{44}$$

Introducing eqs. (34) and (43) into eq. (30), we obtain

$$\delta = \delta_0 \left[1 - \left(\frac{C_T an}{q_R \delta_0}\right)^{\frac{1}{n}}\right] \tag{45}$$

Equation (44) is subject to the initial and boundary conditions given by eq. (40). It is also solved by the Laplace transform to obtain

$$\delta_0^2 = an(n+1)[t-(t-x)u(t-x)] \tag{46}$$

where values of $u\ (t-x)$ are given in eq. (42).

Equations (45) and (46) provide analytical expressions for δ_0 and δ. Equation (43) is useful for the determination of C_b. Equations (29) and (34) provide the information concerning the contaminant distribution in the ROI.

Equations (43), (45) and (46) indicate that when steady state conditions are established in the domain, the ROI starts to develop at $x = x_b$, where

$$\frac{x_b}{a} = \frac{n}{n+1}\left(\frac{C_T}{q_R}\right)^2 \tag{47}$$

It should be noted that eq. (26) provides the following expression for C_b, namely C at $y = 0$

$$C_b = \frac{2q_R}{\sqrt{\pi}}\sqrt{\frac{x}{a}} \tag{48}$$

Considering that at $x = x_b$ the value of C_b is equal to C_T, eq. (48) yields

$$\frac{x_b}{a} = \frac{\pi}{4}\left(\frac{C_T}{q_R}\right)^2 \tag{49}$$

This expression and eq. (47) suggest the adoption of $n = 3$—4 for the TSBL approximation. However, some more significant tests will be performed in the following section for the evaluation of the reliability of the TSBL method for the calculation of contaminant transport in the domain.

Calculations and Results

We have performed numerous comparative calculations aimed at the verification and characterization of the TSBL approach. In the framework of our numerical experiments we have tested the characteristics of all approximate approaches considered in the preceding sections of this report. The hierarchy of the various approximation approaches is used to verify the advantages of the TSBL approach and to show how the improvement provided by the TSBL is adequate and broadens the possible uses of the CBL approximation method. Calculations are presented in two parts. The first part concerns the use of the various approximation methods when the contaminant concentration is prescribed at the free surface of the aquifer. The second part concerns prescribed contaminant mass flux penetrating the free surface of the aquifer.

Prescribed Contaminant Concentration at the Aquifer Free Surface

The dimensionless domain and quantities relevant to this case are shown in fig. 1(a). Contaminant concentration is normalized with regard to the given value of the contaminant

concentration at the aquifer free surface. It is considered that at the ROI the normalized contaminant concentration is higher than 0.01. Therefore the boundary of this region is identified by $C_T = 0.01$.

We apply eq. (15) and calculate changes in the concentration profiles as exemplified by fig. 2. We also have calculated steady state profiles of the contaminant concentration by use of eq. (19) and got profiles identical to those of fig. 2(d) for $t = 100$. The dimensionless length of the simulated region is $x_{max} = 50$, and the build-up of the ROI is completed at $t \approx 100$. Therefore, we may conclude that the build-up requires a time period about twice as long as the time needed for the advection of a fluid particle across the region subject to contamination. We apply the contaminant concentration profile calculations in order to calculate the thickness δ of the region of interest. If the concentration line C_T is located between the ordinates y_1 and y_2, at which $C = C_1$ and $C = C_2$, respectively, we consider that the following power series can be used for the concentration profile between y_1 and y_2.

$$C = (C_1 - C_2)(1-\theta)^n + C_2 \tag{50}$$

where

$$\theta = (y - y_1)/(y_2 - y_1) \tag{51}$$

Consider that

$$C = C_T \quad at \quad y = \delta \tag{52}$$

equations (50) and (51) yield

$$\delta = y_1 + (y_2 - y_1)\left[1 - \left(\frac{C_T - C_2}{C_1 - C_2}\right)^{\frac{1}{n}}\right] \tag{53}$$

Such an approximation has been used for the determination of δ in all numerical simulations performed in the framework of this study.

Calculations of the build-up of the ROI are exemplified by fig. 3. It is noted again that results for $t = 100$ are identical to those referring to steady state conditions. Simulations obtained by use of eq. (15) at $t = 100$ completely converge to those of eq. (19).

Figure 4 shows the build-up of the contaminant concentration profiles according to eq. (22). In these simulations the effect of longitudinal dispersion is neglected. However, concentration profiles in fig. 5 are very similar to those obtained in fig. 2. Figure 4(c) concerns profiles identical to steady state profiles obtained by use of eq. (25). In fig. 5 we compare steady state profiles obtained by use of eq. (19) with those obtained by eq. (25). They are almost identical. The phenomenon of a very minor effect of the longitudinal dispersion on the shape of the concentration profiles has been observed even in cases of $a_L = 100 \cdot a$. However, steady state conditions have been obtained according to eq. (22) in a shorter time period than predicted by use of eq. (15).

Figure 6 shows the build-up of the ROI as predicted by use of eq. (22). As shown the ROI build-up is almost completed at $t = 50 = x_{max}$.

Figure 7 compares the build-up of the ROI with and without consideration of the longitudinal dispersion. Although there are some differences between the steady state values of δ, the build-up processes are very similar.

All data of fig. 4(c) are used to calculate profiles of C versus y/δ_0. Values of δ_0 are identified as locations in which $C \leq 0.001$, namely C is smaller in an order of magnitude than C_T. As shown in fig. 8, all data of fig. 4(c) converge to a single curve by that procedure. The same phenomenon of convergence to a single curve occurs in every set of data obtained by reference to a very wide range of $0.01 \leq a \leq 1.0$ in steady as well as unsteady state conditions. Therefore, it is found sufficient to compare possible values of n, of the power series expansions, with profiles of C versus y/δ_0 in a single cross section. Such comparisons are given in fig. 9. This figure indicates that for the whole range of tested a-values the best fit value for n is about 3. Fig. 9 shows that $n = 2$ is not an appropriate approximation for the description of the contaminant concentration profiles. However, in the framework of the present study we have found that the value of $n = 2$ had been the only one used in previous studies for calculations applying the classical boundary layer (CBL) approach. The CBL does not define the top of the BL with

specific values of C, and considers that at the top of the BL $C \approx 0$. But it is common to consider that $C \approx 0.01$ at that location with no well-defined reason.

In fig. 10 we compare steady state values of δ obtained by use of eq. (25) with those predicted by eqs. (39) and (41), where δ is defined as the ordinate y at which $C = C_T = 0.01$. The CBL approach eventually states that δ_0 is the appropriate value of δ, and $n = 2$ is the common used value for the power series expansion. Fig. 10(a) indicates that the inaccurate assumption of $n = 2$ compensates the inaccurate assumption of $\delta = \delta_0$. Therefore, values of δ_0 obtained by use of $n = 2$ in eq. (41) are quite similar to values of δ obtained by use of eq. (25). However, the assumption of $n = 2$ provides values of δ by use of eq. (39) which are considerably smaller than those obtained by use of eq. (25). The assumption of $n = 2$ also provides inadequate description of the contaminant distribution in the ROI, as indicated by fig. 9.

In fig. 10(b) the same comparison of fig. 10(a) is made with $n = 3$. Values of δ_0 implied by eq. (41) are considerably higher than values of δ obtained by use of eq. (25) and eq. (39). This result indicates that if the value of C_T is not specified, as in the CBL approach, then either values of C are not well correlated with y/δ_0 or values of δ are not well correlated with those implied by the exact solution of the diffusion-advection equation. To obtain good correlation with the C profiles the adopted value of n should be about 3. On the other hand in order to apply the CBL approach and obtain adequate values of δ the adopted value of n should be 2. The TSBL method suggested by this study provides values of δ almost identical to those predicted by eq. (25) when $n = 3$, as shown in fig. 10(b). Therefore, the TSBL approach gives adequate values of δ as well as profiles of C.

In fig. 11 we compare steady state values of δ as implied by all approximations. It seems that values calculated with the TSBL approximation while $n = 3$ are quite well correlated with those obtained both with and without consideration of longitudinal dispersion.

In fig. 12 we compare the rate of growth of δ according to the TSBL approach with the numerical solution given by eq. (22). Both methods predict that the build-up of the ROI is completed at a dimensionless time period approximately equal to x_{max}. Eventually eq. (41)

shows that exactly at $t = x_{max}$ the build-up of the ROI is completed. Such a time period is needed for the advection of a fluid particle along the extent of the contaminated region. It should be noted, as implied by figs. 2 and 3, that the numerical scheme of eq. (15) yields longer build-up time period.

Prescribed Contaminant Flux Penetrating Through the Aquifer Free Surface

In the previous section we applied a hierarchy of approximation solutions of the diffusion-advection equation and showed that the TSBL approach provides better and more accurate description of the contaminant distribution as well as the build-up of the ROI under conditions of prescribed surface concentration. With regard to prescribed contaminant flux penetrating into groundwater through the free surface of the aquifer, the contribution of the TSBL approach can be even more significant as the CBL method is not documented as a method applicable in cases of prescribed flux quantities.

Also in this section we define the ROI as shown in fig. 1(b). It is part of the domain in which the normalized contaminant concentration is larger than 0.01, namely $C_T = 0.01$. However, the value of C_b is subject to changes in time and along the free surface of the aquifer.

We have performed numerous calculations concerning the contamination process as implied by the hierarchy of approximate methods considered in the theoretical background of this report. Some of these calculation results are given graphically in this report.

We apply the numerical scheme of eq. (15) in conjunction with the finite difference approximation of the boundary and initial conditions of eq. (13), and calculate the development of contaminant concentration profiles in groundwater as described in fig. 13. We chose values of a and a_L identical to those of fig. 2. However, changes in concentration profiles and the build-up of the ROI also depend on the value of q_R. At the downstream end of the domain at $t \geq 50$, as shown in figs. 13(b)–(d), C_b obtains values larger than unity. This result stems from the comparatively high rate of the penetrating mass flux, q_R of the contaminant.

Contaminant profiles of fig. 13(d) considering $t = 100$ have been almost identical to steady state concentration profiles obtained by use of eq. (19). This result indicates that the build-up of the ROI is completed in a time period identical to that needed for the build-up of that region when contaminant concentration is prescribed at the aquifer's free surface.

Figure 14 shows the build-up of the ROI as predicted by use of eq. (15) and the boundary conditions of eq. (13). It should be noted that due to the comparatively high value of q_R, fig. 14 shows that δ starts to develop at a very short distance from the leading edge of the domain, namely $x_b \approx 0$. In following calculations and examples we provide more details about high and small values of q_R.

Figure 15 shows the development of C_b in time and along the free surface of the aquifer according to eq. (15) and the boundary conditions of eq. (13). Again, due to the comparatively high value of q_R, the value of C_b is larger than 0.01 even in close proximity to the leading edge of the simulated domain. However, as will be shown in some other examples concerning low values of q_R and high values of a, at a range of $0 \le x \le x_b$, the value of C_b is smaller than 0.01 and δ vanishes.

In the next stage we have made numerous simulations in which longitudinal dispersion has been neglected. Practically, results concerning the build-up of the concentration profiles as well as values of δ and C_b have been almost identical to those obtained when longitudinal dispersion was considered, even in cases of $a_L \approx 100 \cdot a$. From all these calculations we show in fig. 16 the steady state profiles of C and compare some of these profiles with those obtained by use of eq. (19). Fig. 16(b) shows that profiles obtained by use of eq. (26), in which a_L is neglected, are almost identical to those obtained by use of eq. (19), in which a_L is considered.

We have performed numerous calculations similar to those presented in fig. 16 as well as in intermediate stages. However, basically all these calculations have been coherent with the steady state observations shown in figs. 16–18.

In fig. 17 we exemplify some of the tests carried out in the framework of evaluation of the possible correlation between C/C_b and y/δ_0. From the obtained tables of concentration

profiles represented in fig. 16(a) and similar figures which are not given in this report we observed for each cross section the value of δ_0 in which $C/C_b \leq 0.001$, provided that $C_b < 1$. If C_b in parts of the domain has been larger than 1, then smaller values of C/C_b have been considered for δ_0 in order that for all values of δ_0 the relationship of $C \leq 0.1\ C_T$ was preserved. Following the identification of the domain, profiles of C/C_b versus y/δ_0 have been depicted. Fig. 17 shows some of the results. This figure indicates that for the whole domain, for each tested set of the basic parameters q_R and a, the relationship between C/C_b and y/δ_0 is preserved. However, another set of tests is needed in order to identify the effect of variability of q_R and a on the relationship between C/C_b and y/δ_0. Such tests have been performed. Some of the results are shown in fig. 18. This figure indicates that the best fit value of n depends upon the value of q_R/a. Such a result probably stems from the identity of this parameter to the vertical gradient of the concentration profile at $y = 0$. Figs. 18(a) and 18(c) refer to very different values of q_R and a, but identical q_R/a. Both of them suggest the use of $n = 3$. Figs. 8(b) and 8(d) by the same principle imply $n = 4$. These results indicate that the optimum value of n increases moderately with the increase in q_R/a.

In fig. 19 we provide a comparison between steady state values of δ and δ_0 obtained by the TSBL approximation, namely eqs. (45) and (46), and the value of δ obtained by using eq. (26). Values of δ obtained by both methods are almost identical. It should be noted that differences between values of δ_0 in figs. 19(a) and 19(b) originate only from difference in values of a, as implied by eq. (46), whereas differences between values of δ in these figures originate from values of a as well as q_R. The definition of δ_0 is solely dependent on C/C_b values whereas δ is defined by C_T, which is a concentration normalized with regard to a constant characteristic quantity, C_0.

Because the value of q_R in fig. 19(b) is much smaller than in fig. 19(a), there is a region, extended up to x_b, in fig. 19(b), where there is no ROI, namely $\delta = 0$ at $0 \leq x \leq x_b$.

Figure 20 concerns the build-up, in time and along the free surface of the aquifer, of C_b. We present in this figure only steady state values of this parameter. However, basic phenomena

are identical to steady as well as unsteady states. Values of C_b obtained by the TSBL approximation namely eq. (43) are almost identical to those of eq. (48). The latter is derived from the analytical solution given by eq. (26). Values of C_b in curves B are much smaller than those of curves A due to the significant differences in values of q_R.

Figure 21 shows the development of δ in time and space. Values in this figure are calculated by the TSBL method, namely eqs. (45) and (46), as well as the numerical scheme of eq. (22). Very minor differences in values of δ have been obtained between the two methods. The build-up of the ROI, as predicted by both methods, is completed in a time period equal to the time period of advection of a fluid particle along the whole extent of the domain. This is an approximate outcome of using eqs. (45) and (46). If a_L is considered, then the build-up of the ROI is completed in a longer time period, as indicated by fig. 14.

Discussion

This study provides review and calculations of contaminant penetration and transport in a free surface aquifer. However, its major theme concerns the development and use of the TSBL approach.

The CBL approximation is widely used as an initial means for the evaluation of flow and transport phenomena. Basically this approach represents an integral method for the solution of partial differential equations. The CBL approximation has proved to be a convenient method for the evaluation of heat and mass transfer in groundwater provided that the physical problem involves prescribed boundary values for the transported quantity. Referring to contamination of a free surface aquifer, the CBL approach can be proved to be useful provided that the contaminant concentration is prescribed at the free surface of the aquifer. There are some typical cases for an application, such as contamination of the aquifer originating from a floating lens of non-aqueous-phase-liquid (NAPL). The oil (NAPL) lens releases miscible fractions into the underlying aquifer. Probably groundwater which is in direct contact with that lens is saturated with those miscible fractions. It seems, however, that large scale contamination of free surface

aquifers, like contamination by nitrates, pesticides, herbicides, etc., is likely to be better described by prescribed flux at the free surface of the aquifer.

The CBL approximation is not documented as a tool for the simulation of transport phenomena in prescribed surface flux cases. The objective of this study was originally aimed at the extension of the CBL approximation to prescribed surface flux. However, the set of tests, calculations and analyses with the CBL approach indicate that this approach also lacks some important coherencies in cases of prescribed contaminant concentration at the free surface of the aquifer. Results show that the order of the power series considered for the approximation of the contaminant concentration in the boundary layer region should be carefully considered, as it has a very significant effect on the predicted rate of growth in time and space of the BL region. Use of a second order power series, as is usually done, provides according to the CBL a reasonable approximation for the rate of growth of the BL region, but fails to describe adequately the contaminant concentration profiles within the region. Adoption of a third order power series approximation provides an adequate means for the description of the profiles of contaminant concentration in the boundary layer region, but fails to predict accurately the rate of growth of this region.

It seems that the difficulties involved in use of the CBL approach originate from the lack of specification of the upper edge, top, of the boundary layer region. The definition of "vanishing contaminant concentration" is inappropriate, mainly in environmental problems, where contaminant concentrations of ppbs are sometimes very significant. Therefore, the definition of zero contaminant concentration at the top of the boundary layer is replaced by "acceptable value" of that parameter. Practical interest is associated with the ROI, where contaminant concentration exceeds the acceptable value. It is also suggested to normalize contaminant concentrations in the domain with regard to a concentration that is about 100 times larger than the acceptable value. The specification of the range of contaminant concentration included in the BL, namely the definition of the ROI, represents the major contribution of this study. As a result of this basic improvement of the CBL approach, we have succeeded in

obtaining adequate descriptions of contaminant concentration profiles in the ROI and adequate predictions of the rate of growth of the contaminated region.

The TSBL approach permits simulation of groundwater contamination when fluxes of the contaminant penetrating through the aquifer's free surface are prescribed.

All calculations presented in this study refer to idealized aquifers of very large extent with uniform velocity distribution, flow parameters, etc. In such a system the applicability of the TSBL approximation could conveniently be evaluated. However, uses of the TSBL approximation can easily be extended to a variety of non-uniformities in the aquifer and the groundwater system.

Summary

The top specified boundary layer (TSBL) approximation is developed for the calculation of aquifer contamination by contaminants penetrating into groundwater through the aquifer's free surface. The method seems to be very attractive when Dupuit approximation is applied for the description of flow conditions in the aquifer. In the framework of this study it is found that some improvements are needed in order to increase the reliability and range of uses of the classical boundary layer (CBL) approximation to environmental issues. Such improvements are provided by the TSBL approach. According to this method the BL represents a region of interest (ROI) in which contaminant concentration exceeds its acceptable value. The method provides an adequate information about the rate of growth in time and space of the ROI, as well as the distribution of contaminants in that region. The TSBL approach is useful in cases with prescribed contaminant concentration as well as contaminant flux at the aquifer free surface.

The results of this study provide simple but robust approaches to the initial characterization of contamination processes taking place in free surface aquifers.

References

Bachmat, Y. and Bear, J., 1964. The general equations of hydrodynamic dispersion in homogeneous isotropic porous mediums, Journal of Geophysics Research, 69(12):2561-2567.

Carslaw, H.S. and Jaeger, J.C., 1959. "Conduction of Heat in Solids," 2nd ed., Oxford at the Clarendon press, London, U.K. p. 63, 75.

Cole, J., 1968. "Perturbation Methods in Applied Mathematics," Blaisdell, Waltham, Massachusetts.

Dagan, G., 1971. Perturbation solutions of the dispersion equation in porous mediums, Water Resources Research, 7:135.

Eldor, M. and Dagan, G., 1972. Solutions of hydrodynamic dispersion in porous media, Water Resources Research, 8:1316.

Gelhar, L.W. and Collins, M.A., 1971. General analysis of longitudinal dispersion in nonuniform flow, Water Resources Research, 7:1511.

Hunt, B., 1978. Dispersion calculations in nonuniform seepage, Journal of Hydrology, 36:261.

Lapidus, L. and Pinder, G.F., 1982. "Numerical Solution of Partial Differential Equations in Science and Engineering," John Wiley & Sons, New York.

McElwee, C. and Kemblowski, M., 1990. Theory and application of an approximate model of saltwater upconing in aquifers, Journal of Hydrology, 115:139–163.

Ozisik, M.N., 1980. "Heat Conduction," Wiley-Interscience, New York, p. 335.

Rubin, H., 1983. On the application of the boundary layer approximation for the simulation of density stratified flows in aquifers, Advances in Water Resources, 6:96–105.

Rubin, H. and Pinder, G.F., 1977. Approximate analysis of upconing, Advances in Water Resources, 1:97–101.

Rubin, H. and Pistiner, A., 1986. Modeling fresh water injection into a partially saline partially fresh (PASPAF) aquifer, Journal of Hydrology, 37:351–378.

Schlichting, H., 1968. "Boundary Layer Theory," 6th ed., McGraw-Hill, New York, p. 335.

Van Dyke, M., 1964. "Perturbation Methods in Fluid Mechanics," Academic Press, New York.

Wooding, R.A., 1963. Convection in a saturated porous medium at large Rayleigh number or Péclet number, Journal of Fluid Mechanics, 15:527.

Wooding, R.A., 1964. Mixing layer flows in a saturated porous medium, Journal of Fluid Mechanics, 19:103.

Wooding, R.A., 1971. Groundwater problems of the interaction of saline and freshwater, in "Salinity and Water Use," Talsma T. and Philip, J.R. (eds.), Wiley-Interscience, New York, p. 125.

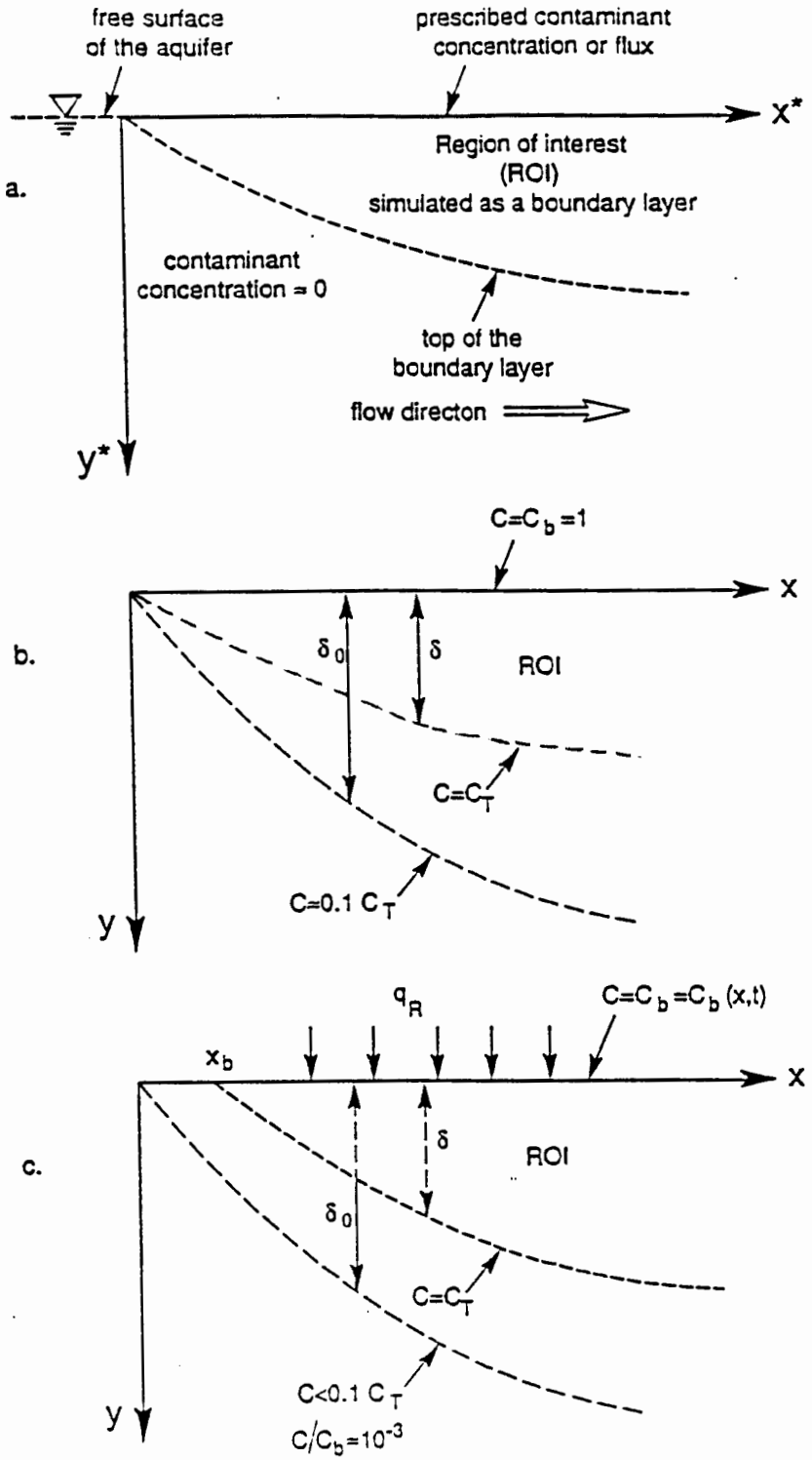

Fig. 1 The conceptual model of the aquifer subject to contamination

(a) Regions of classification

(b) Definition of dimensionless quantities when contaminant concentration is prescribed at $y = 0$

(c) Definition of dimensionless quantities when contaminant flux is prescribed at $y = 0$

Fig. 2 Build-up of the contaminant concentration profiles in space and time as obtained by use of eq. (15) ($a = 0.5$, $a_L = 5$).

(a) $t = 25$;

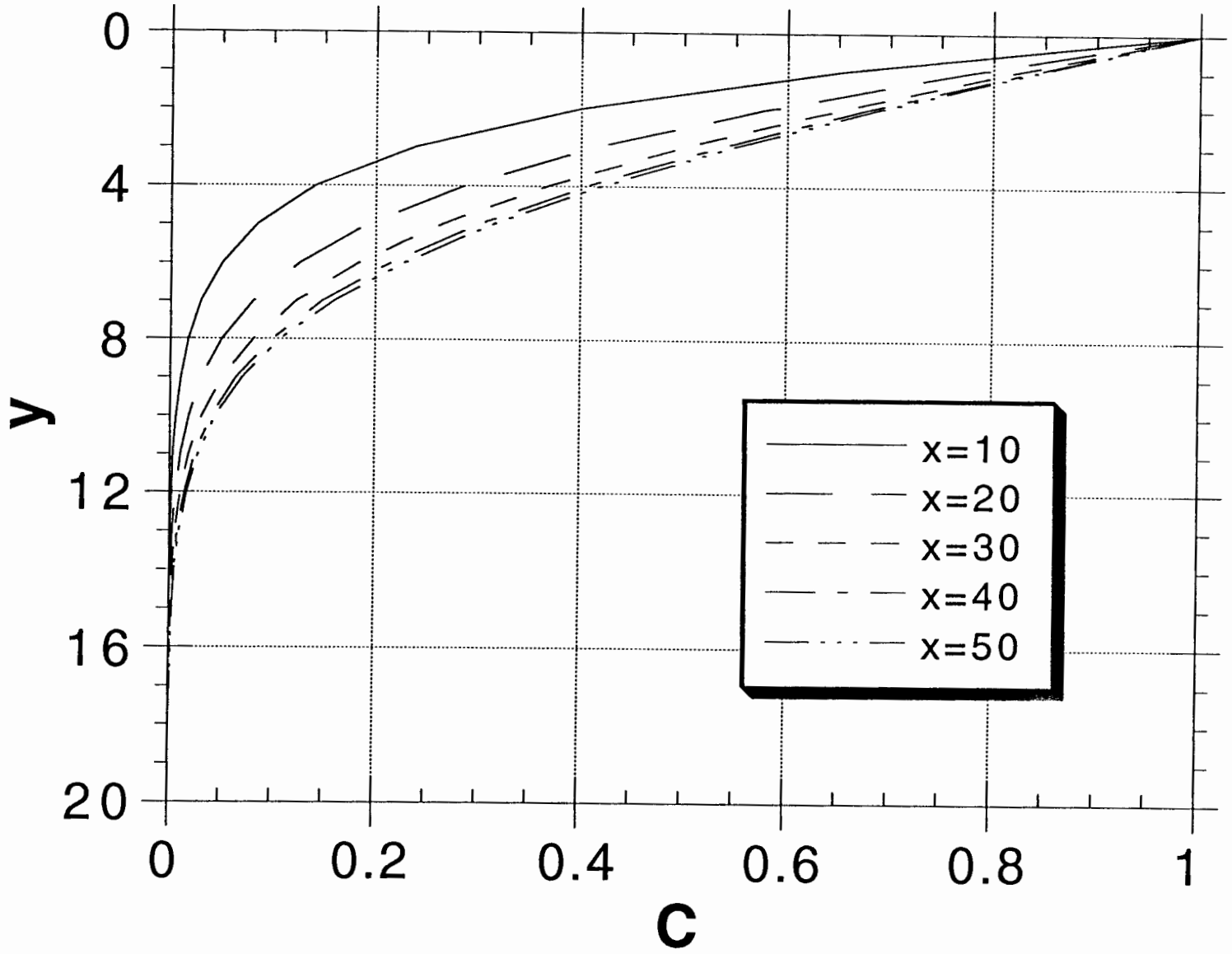

Fig. 2 Build-up of the contaminant concentration profiles in space and time as obtained by use of eq. (15) ($a = 0.5$, $a_L = 5$).

(b) $t = 50$;

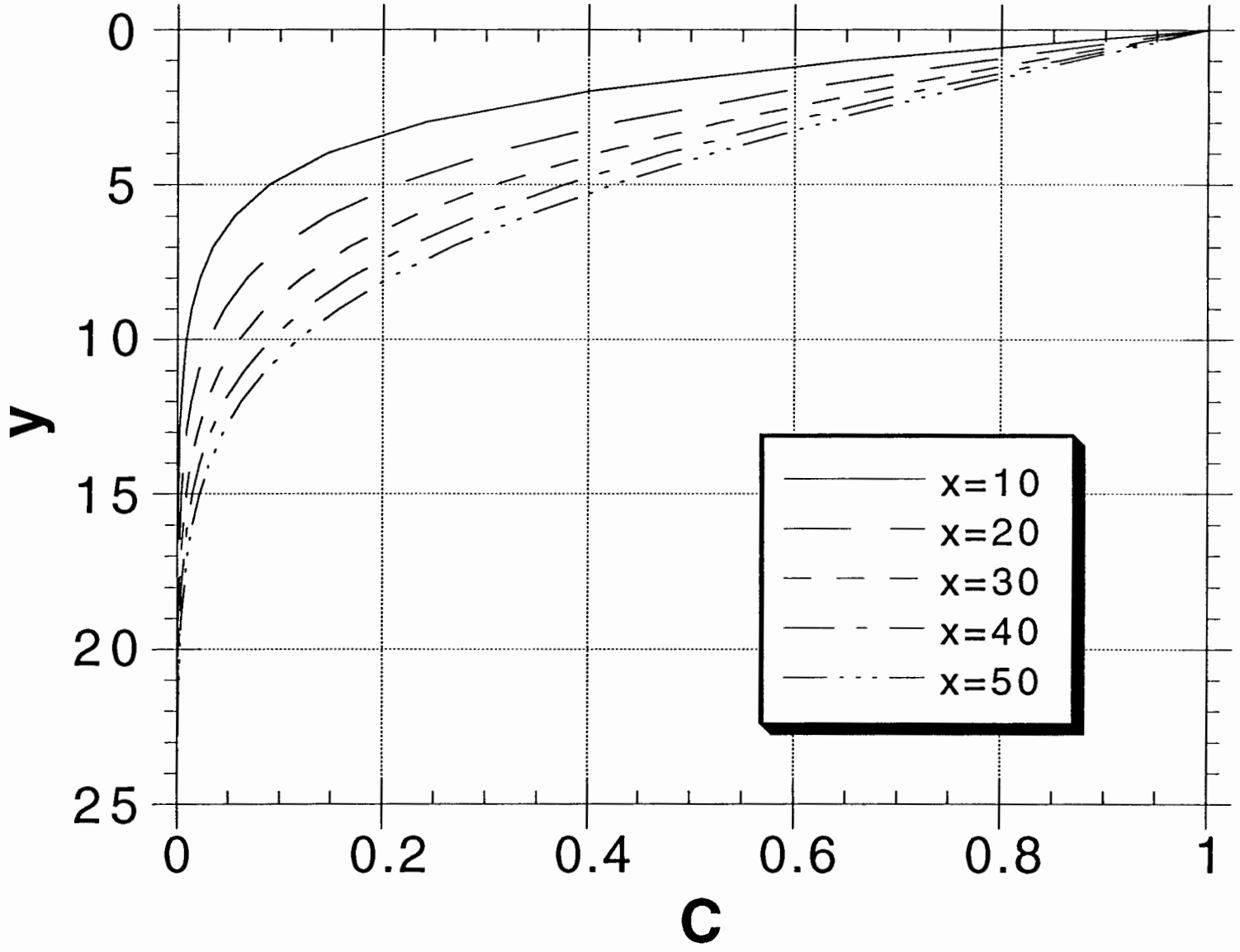

Fig. 2 Build-up of the contaminant concentration profiles in space and time as obtained by use of eq. (15) ($a = 0.5$, $a_L = 5$).

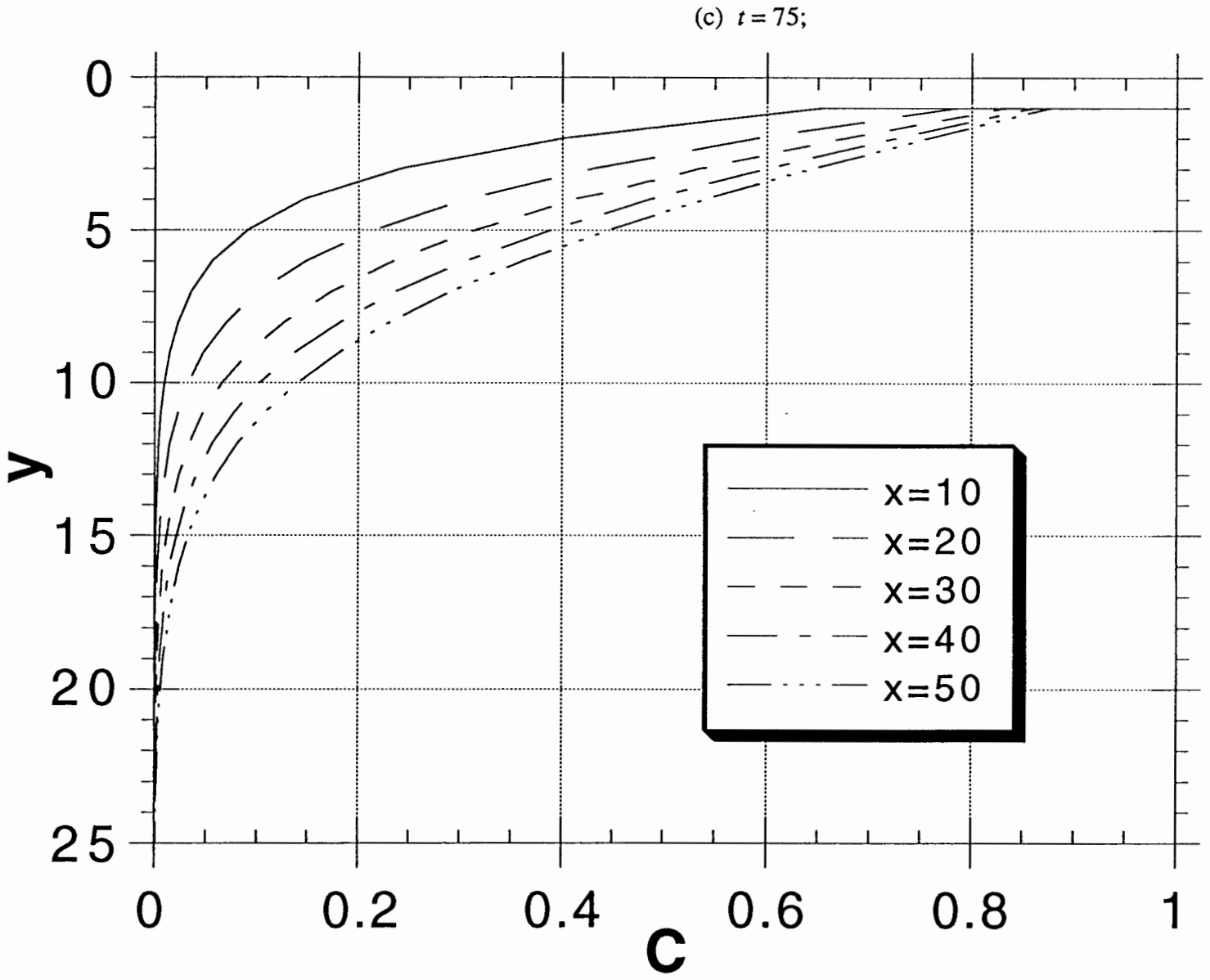

Fig. 2 Build-up of the contaminant concentration profiles in space and time as obtained by use of eq. (15) ($a = 0.5$, $a_L = 5$).

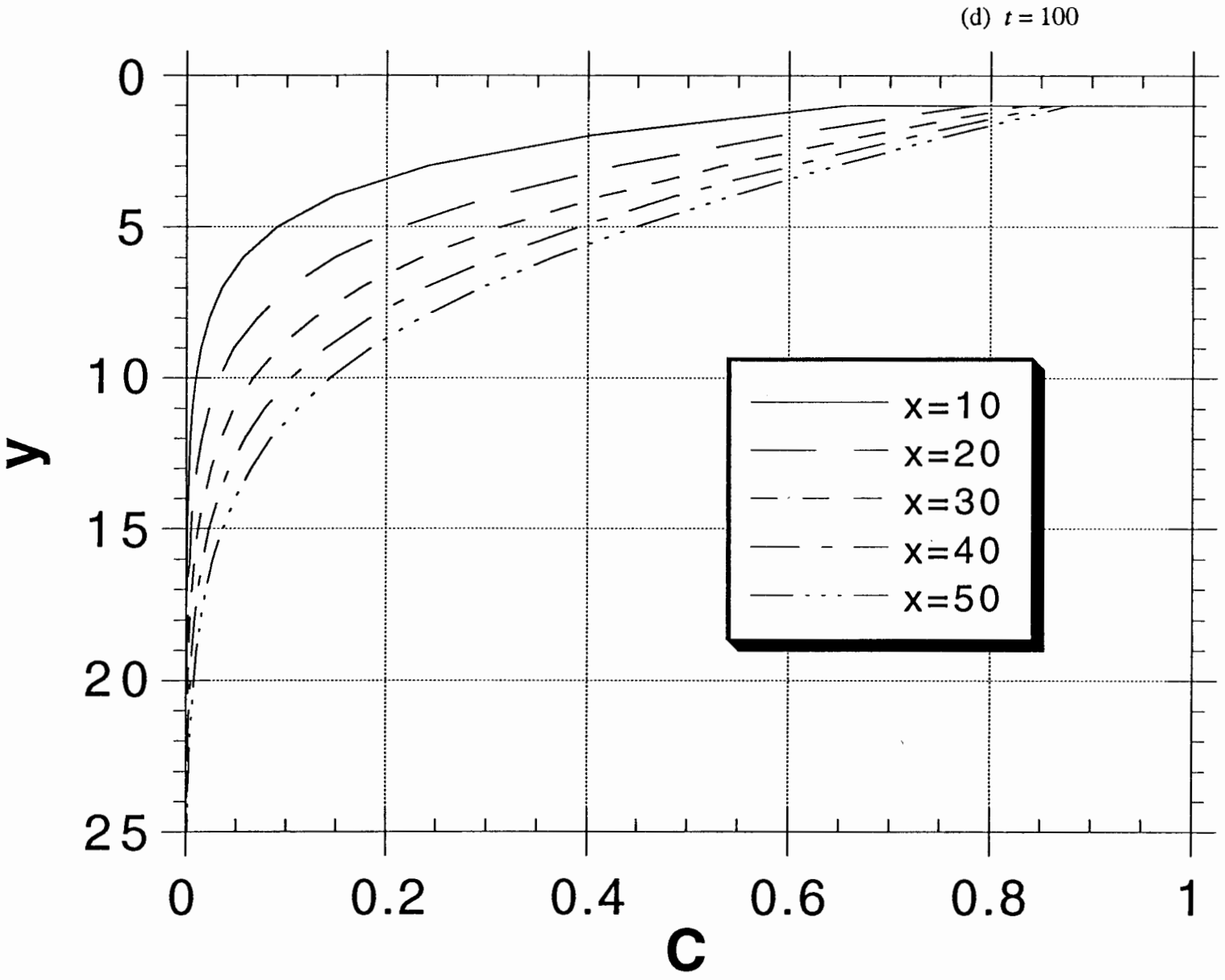

Fig. 3 Build-up of the ROI derived from eq. (15) ($a = 0.5$, $a_L = 5$).

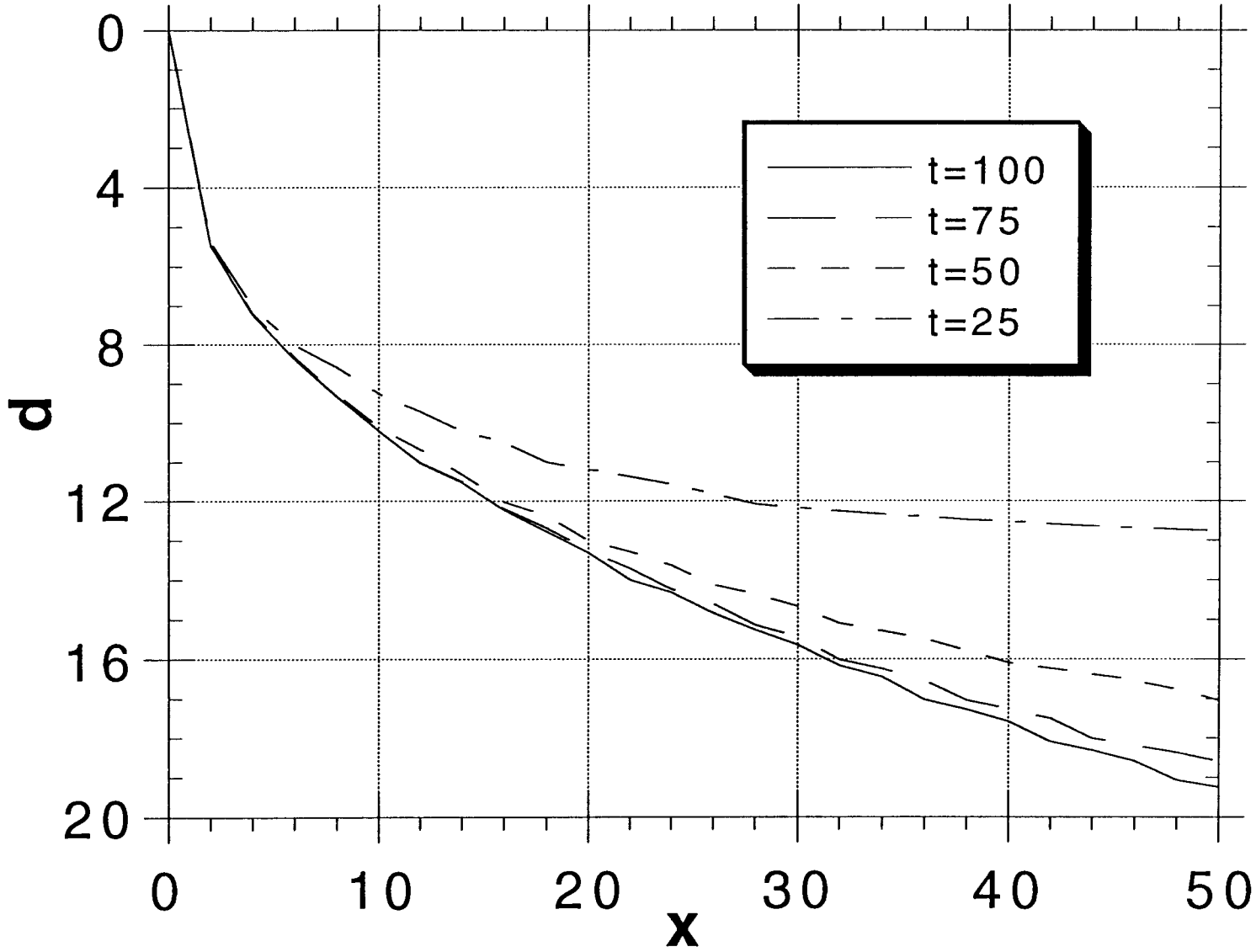

Fig. 4 Build-up of the contaminant concentration profiles in space and time as obtained by use of eq. (22) (a = 0.5).

(a) t = 25;

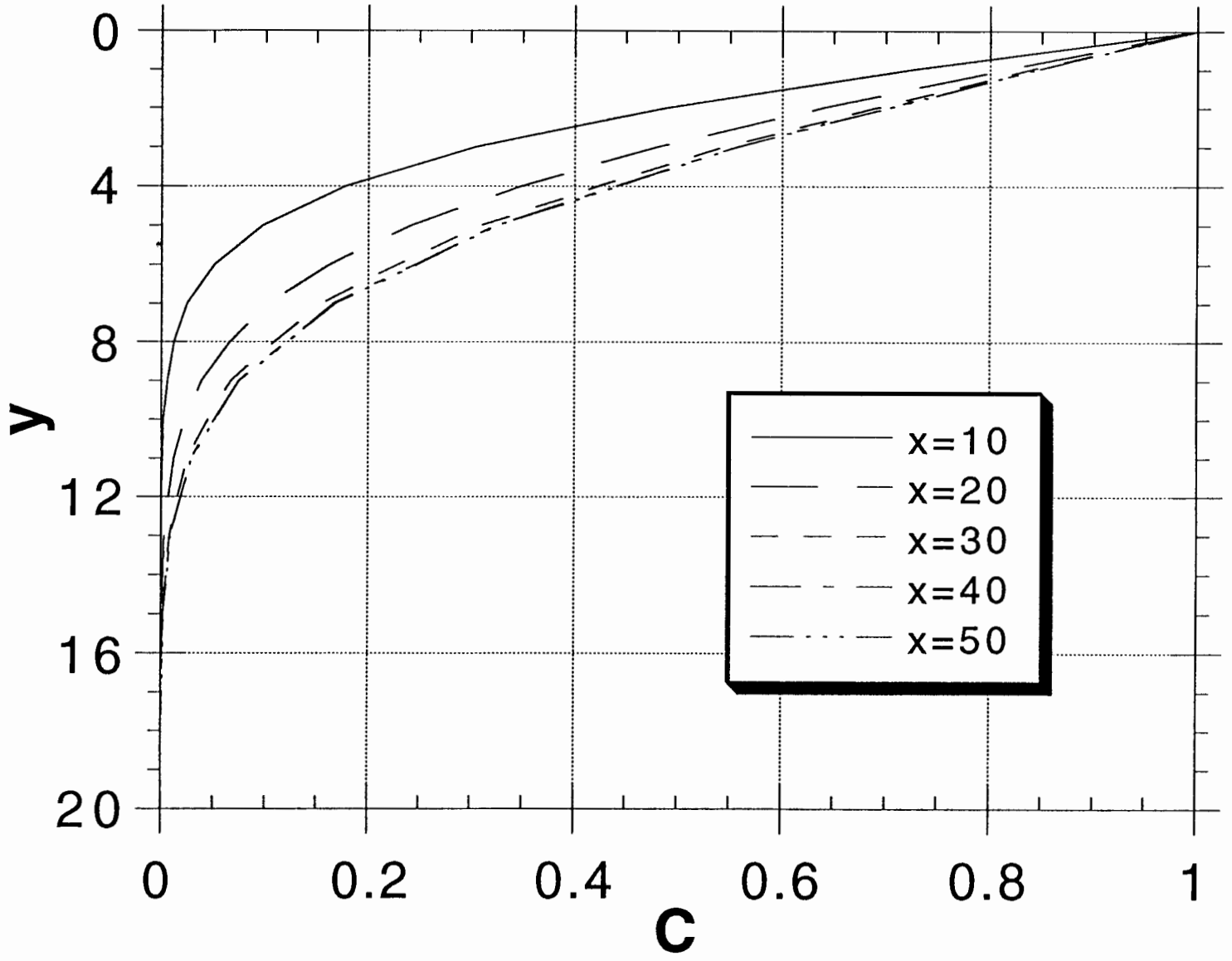

Fig. 4 Build-up of the contaminant concentration profiles in space and time as obtained by use of eq. (22) (a = 0.5).

(b) t = 50;

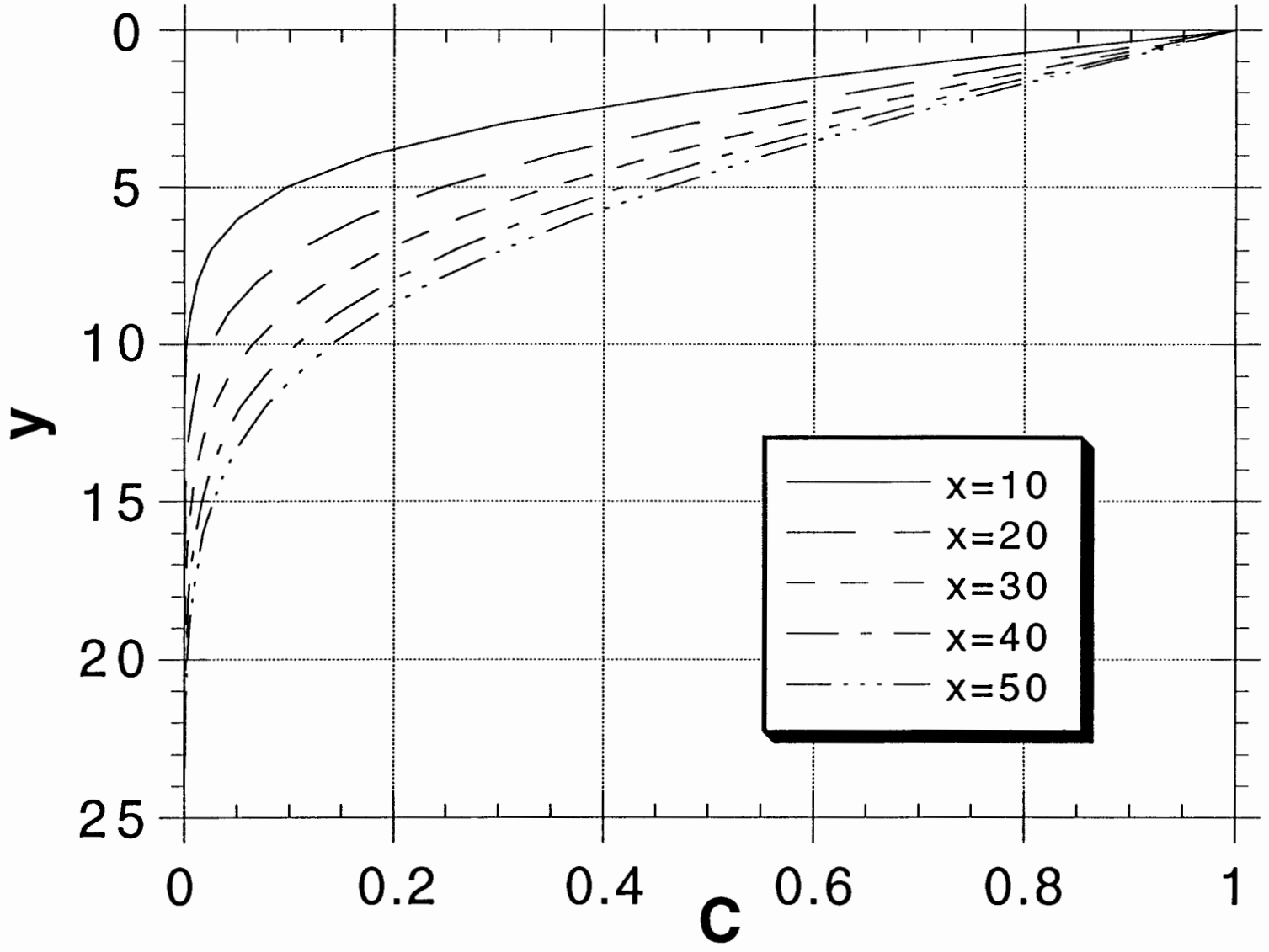

Fig. 4 Build-up of the contaminant concentration profiles in space and time as obtained by use of eq. (22) (a = 0.5).

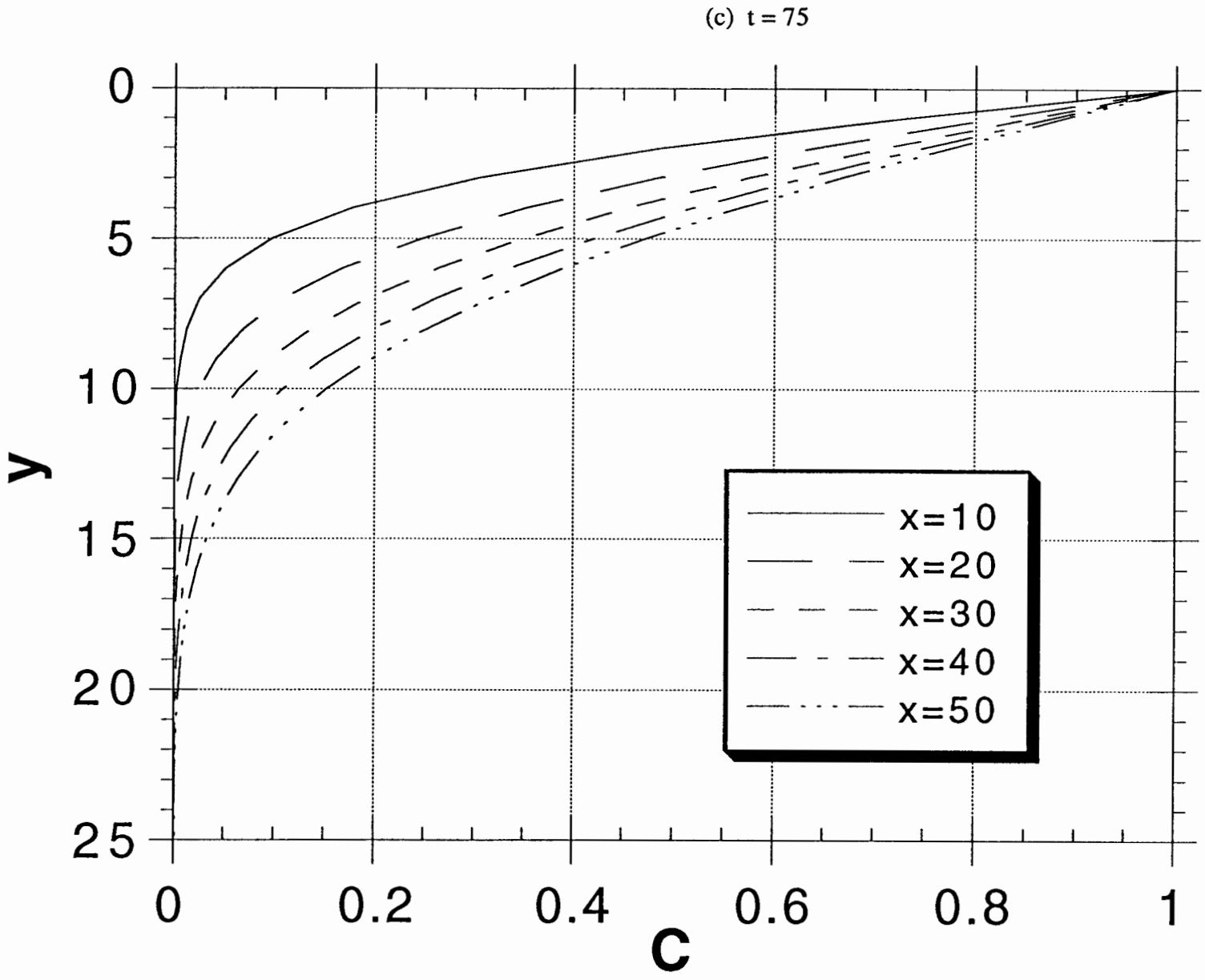

Fig. 5 Comparison between steady state contaminant concentration profiles obtained by use of eq. (19) and those obtained by eq. (25) ($a = 0.5$, $a_L = 5$).

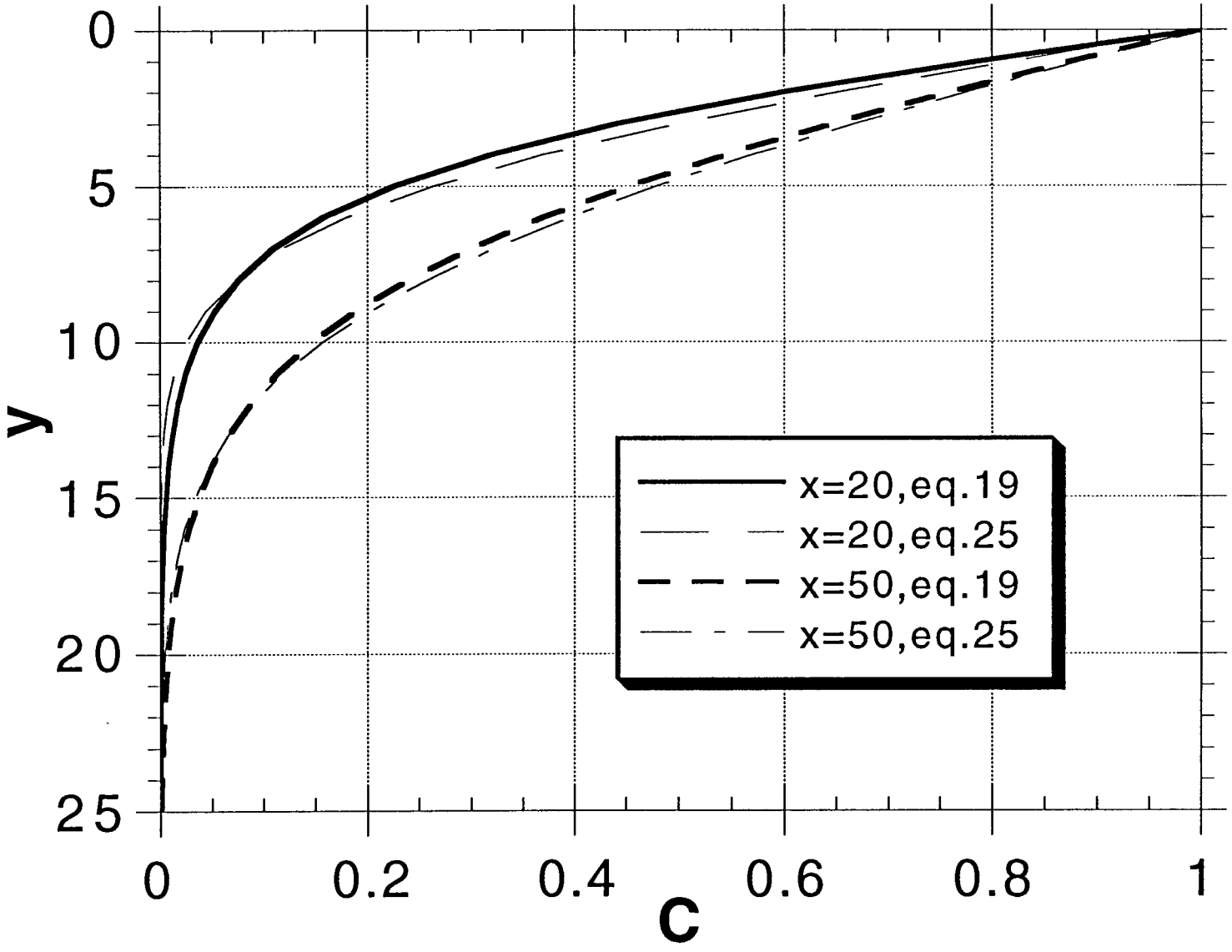

Fig. 6 Build-up of ROI derived from eq. (22) ($a = 0.5$).

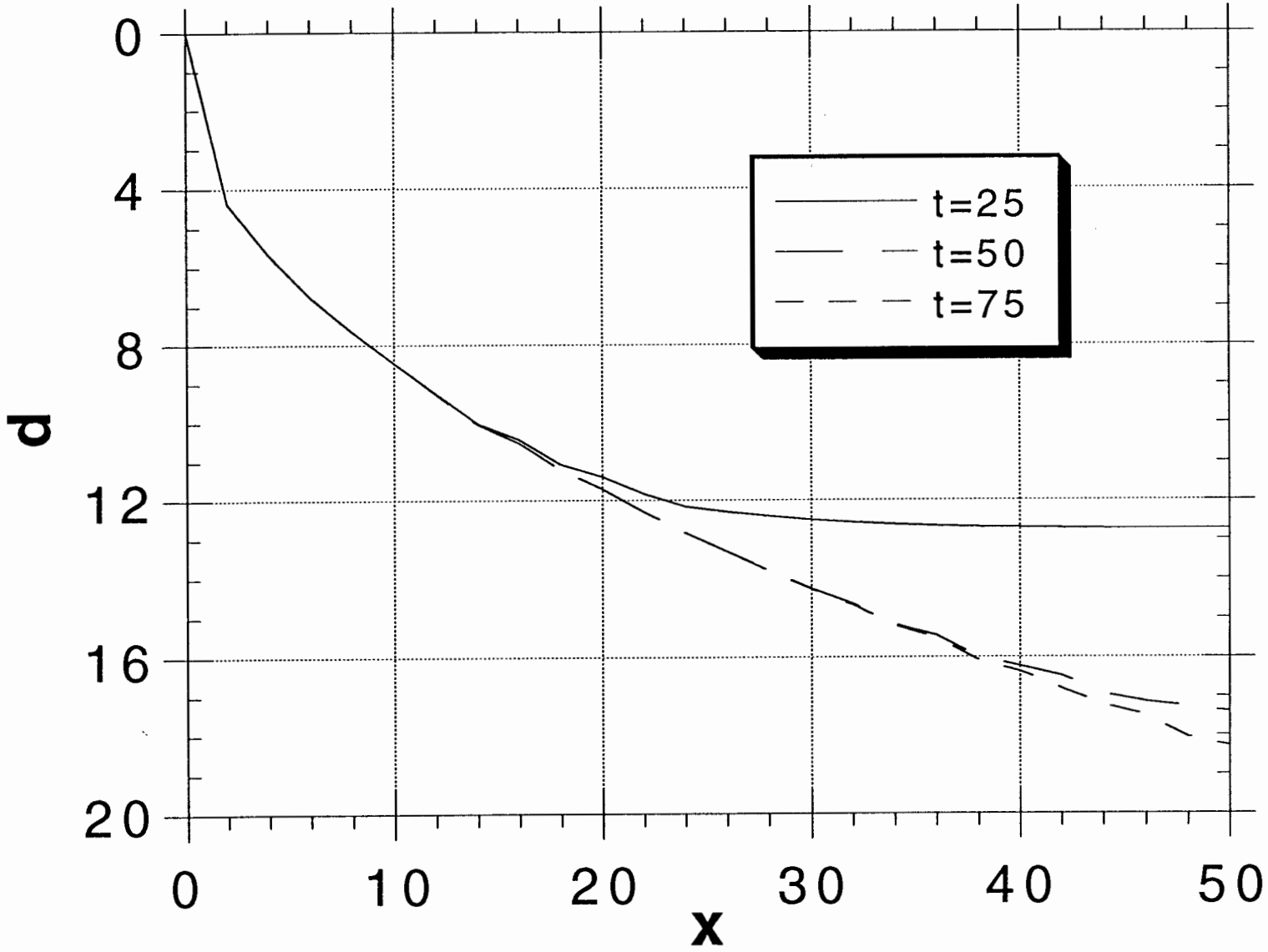

Fig. 7 Comparison of intermediate ($t = 25$) and steady state values of δ obtained with [eqs. (15), (19)] and without consideration [eqs. (22), (25)] of longitudinal dispersion ($a = 0.5$, $a_L = 5$).

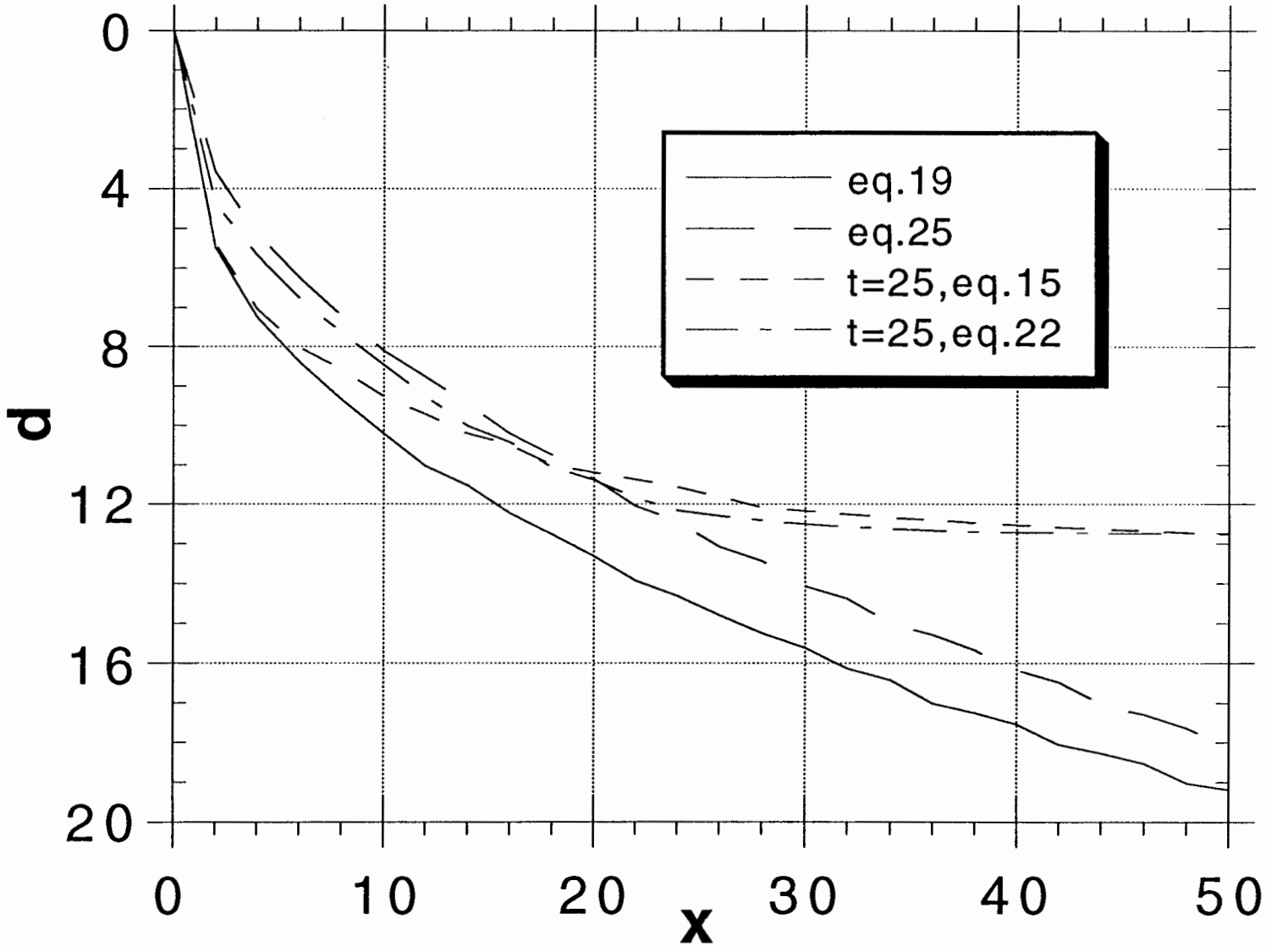

Fig. 8 Steady state profiles of C versus y/δ_0 ($a = 0.5$).

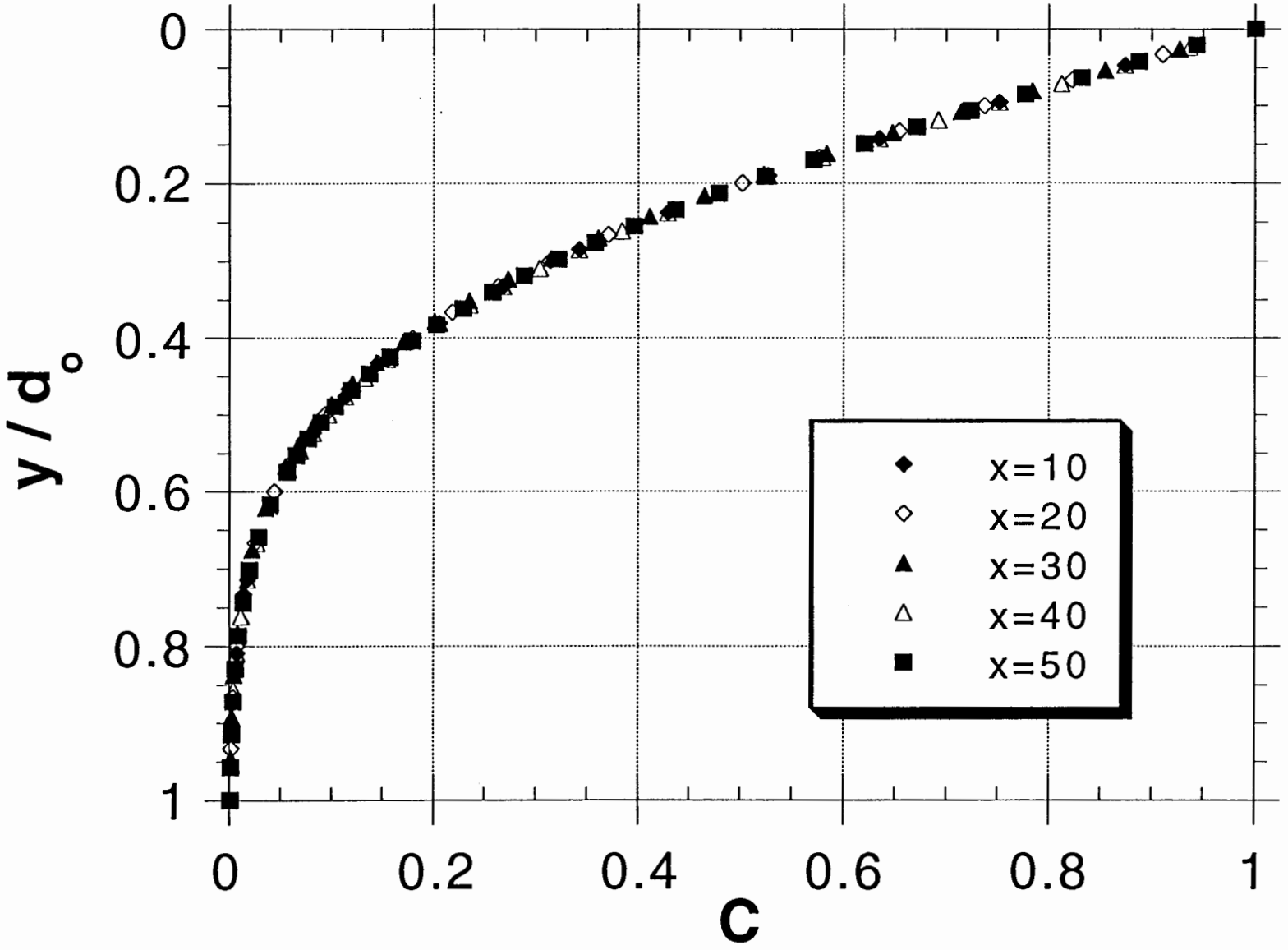

Fig. 9 Comparison between steady state profiles of C versus y/δ_0 according to eq. (25) at x = 50 and various power series expansions.

(a) $a = 0.01$;

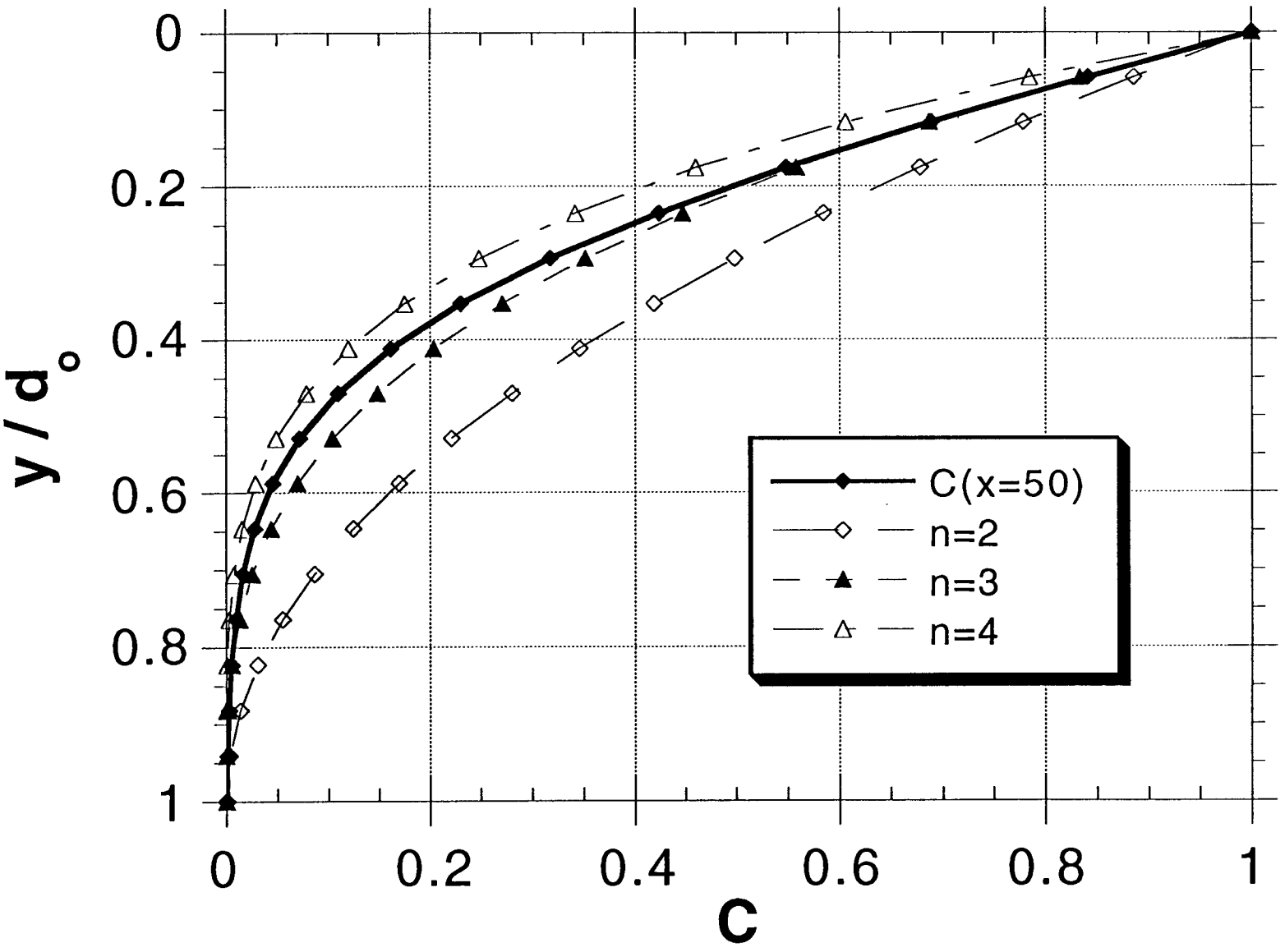

Fig. 9 Comparison between steady state profiles of C versus y/δ_0 according to eq. (25) at x = 50 and various power series expansions.

(b) $a = 0.1$;

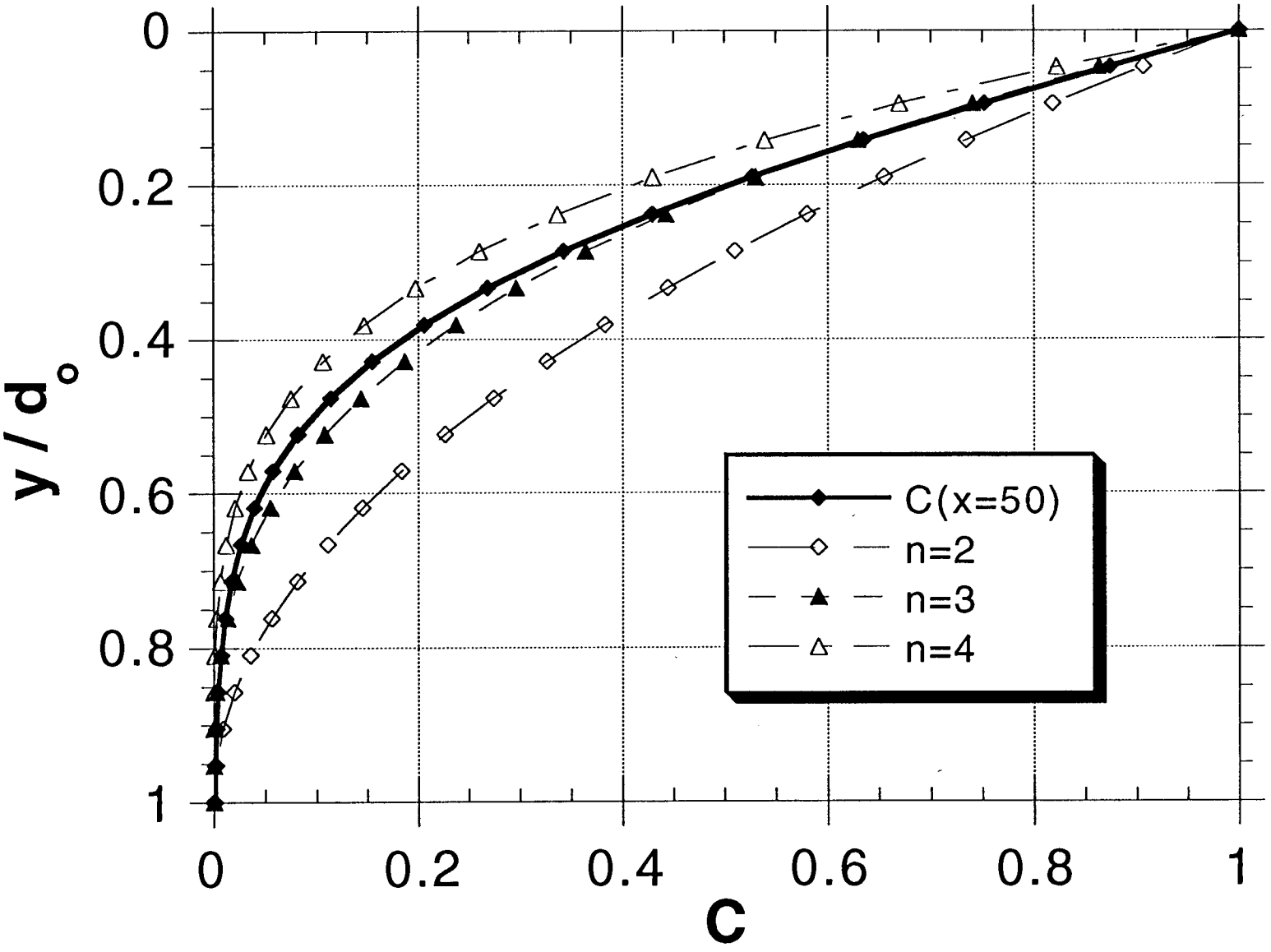

Fig. 9 Comparison between steady state profiles of C versus y/δ_0 according to eq. (25) at x = 50 and various power series expansions.

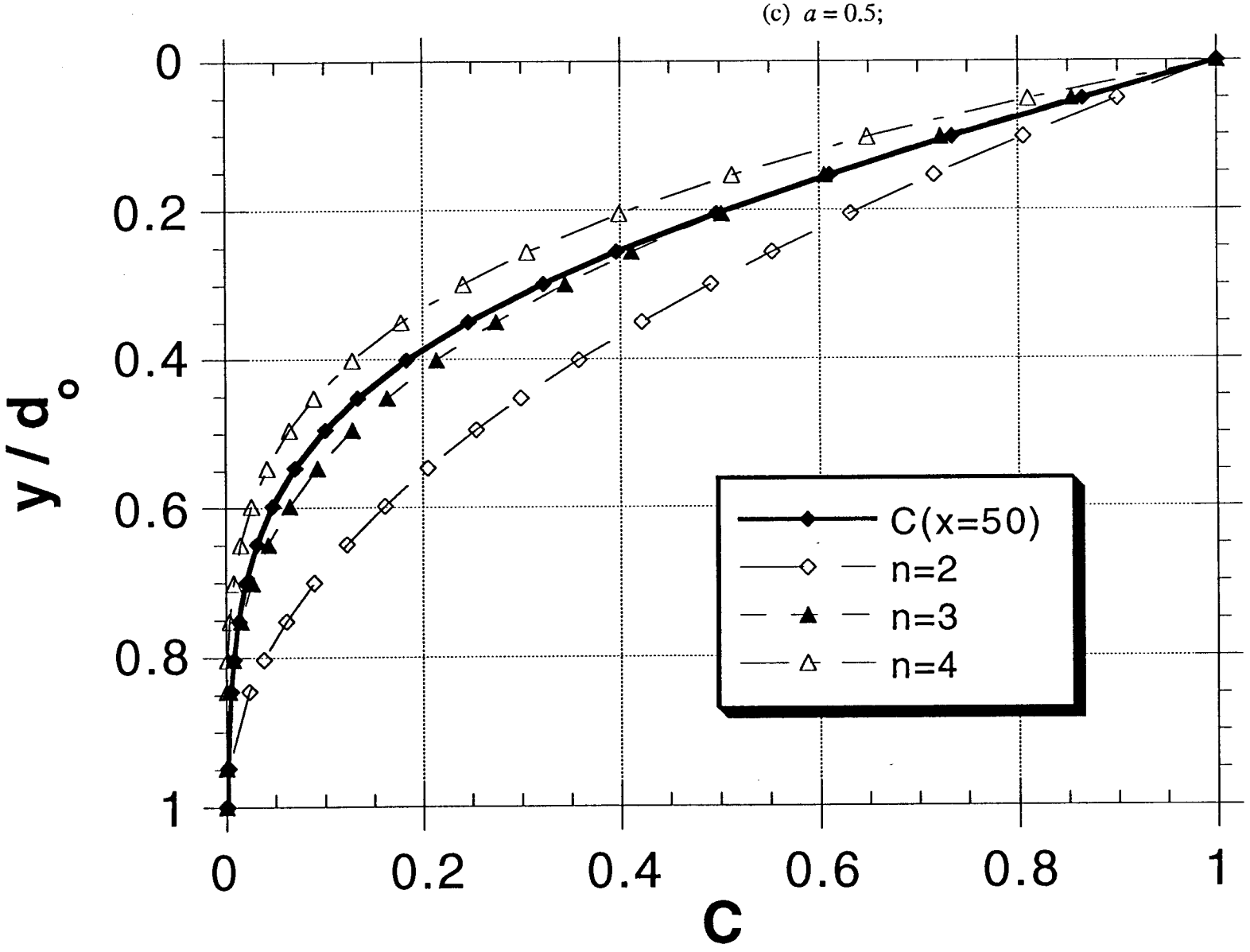

Fig. 9 Comparison between steady state profiles of C versus y/δ_0 according to eq. (25) at x = 50 and various power series expansions.

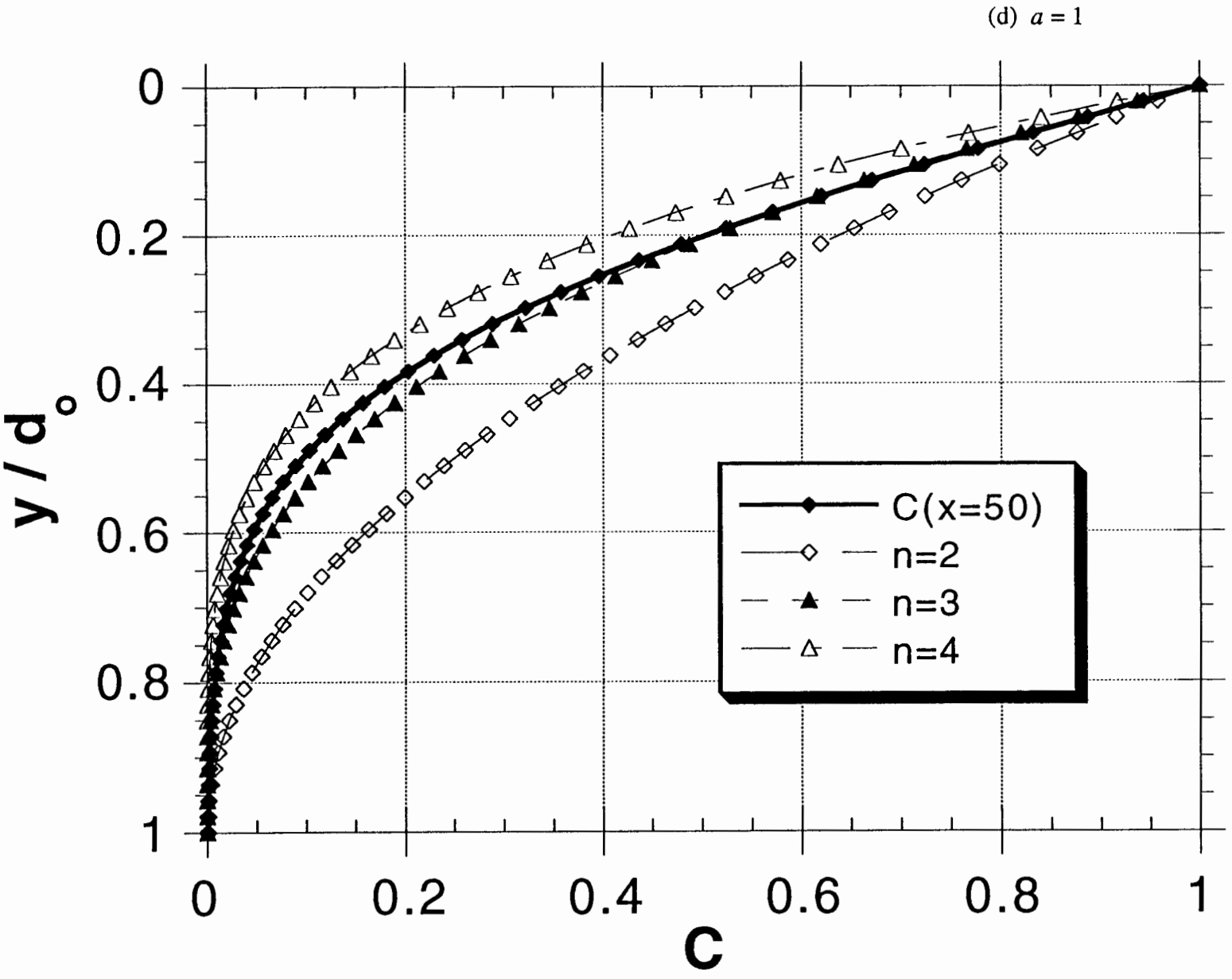

Fig. 10 Comparison between steady state values of δ and δ_0 obtained by the TSBL approach and values of δ obtained by eq. (25) ($a = 0.5$).

(a) $n = 2$;

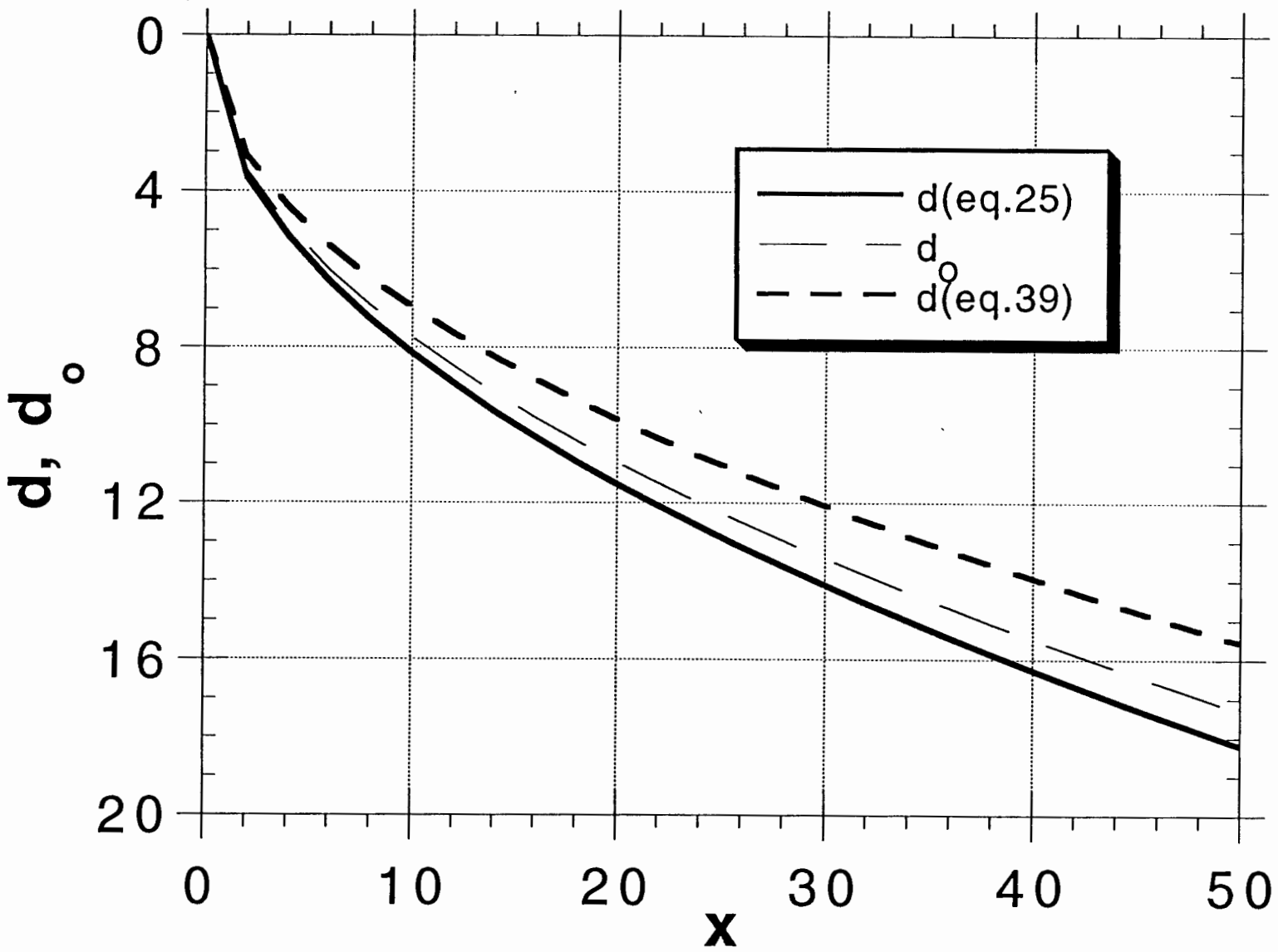

Fig. 10 Comparison between steady state values of δ and δ_0 obtained by the TSBL approach and values of δ obtained by eq. (25) ($a = 0.5$).

(b) $n = 3$

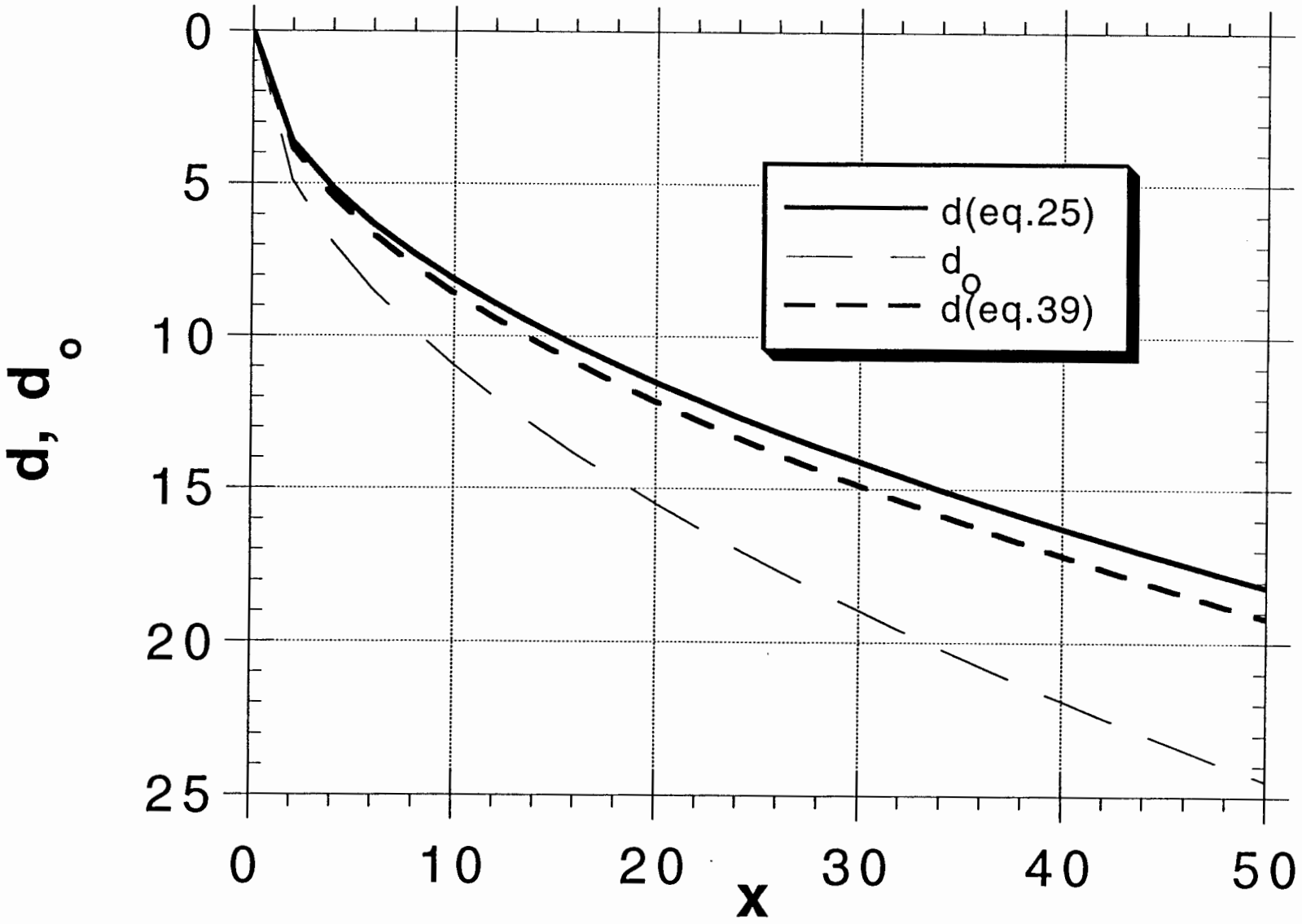

Fig. 11 Steady state values of δ according to all approximations ($a = 0.5$, $a_L = 5$, $n = 3$).

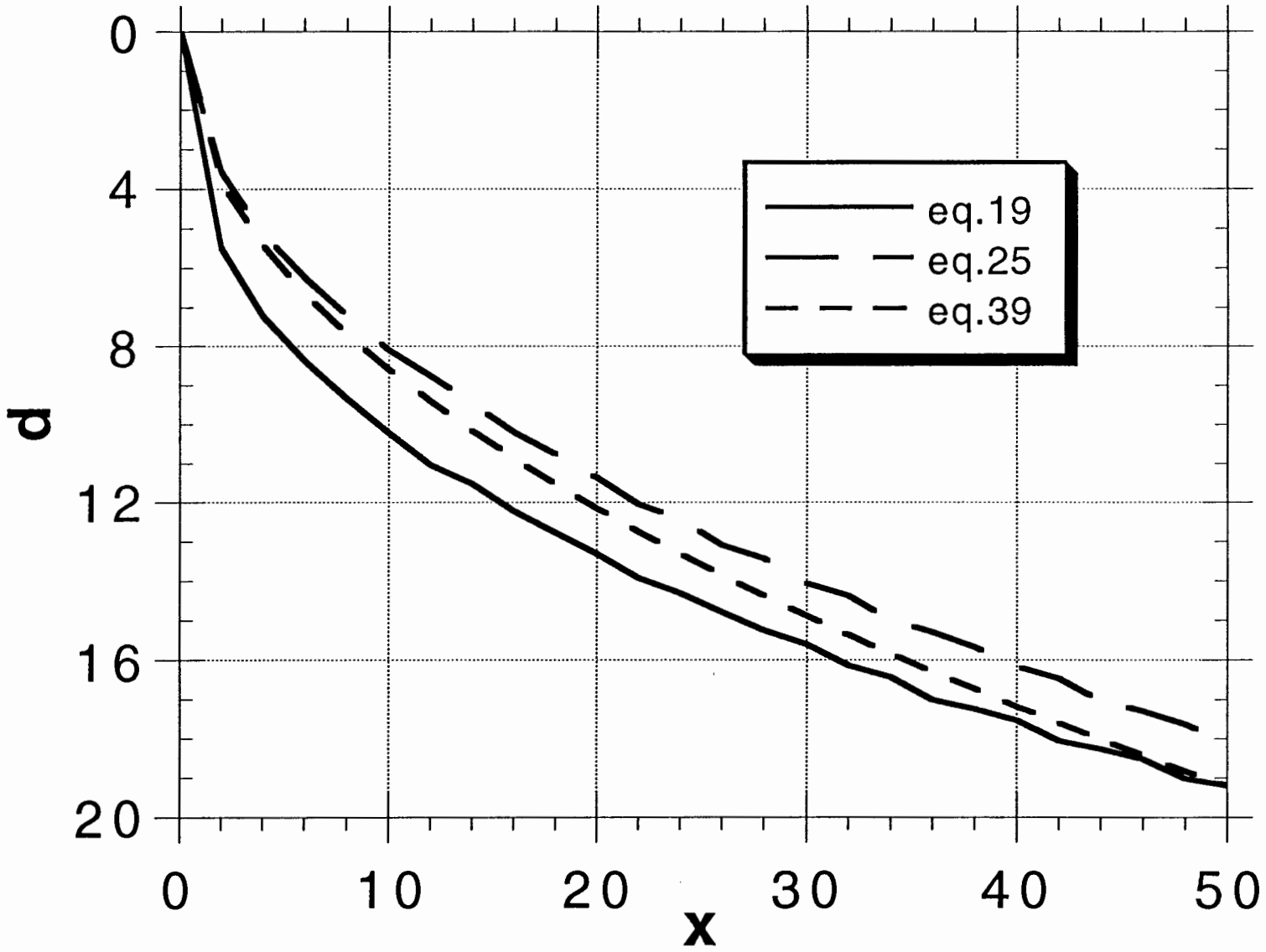

Fig. 12 Comparison between values of δ according to eq. (22) and the TSBL method [eqs. (39, (41)] ($a = 0.5$, $n = 3$).

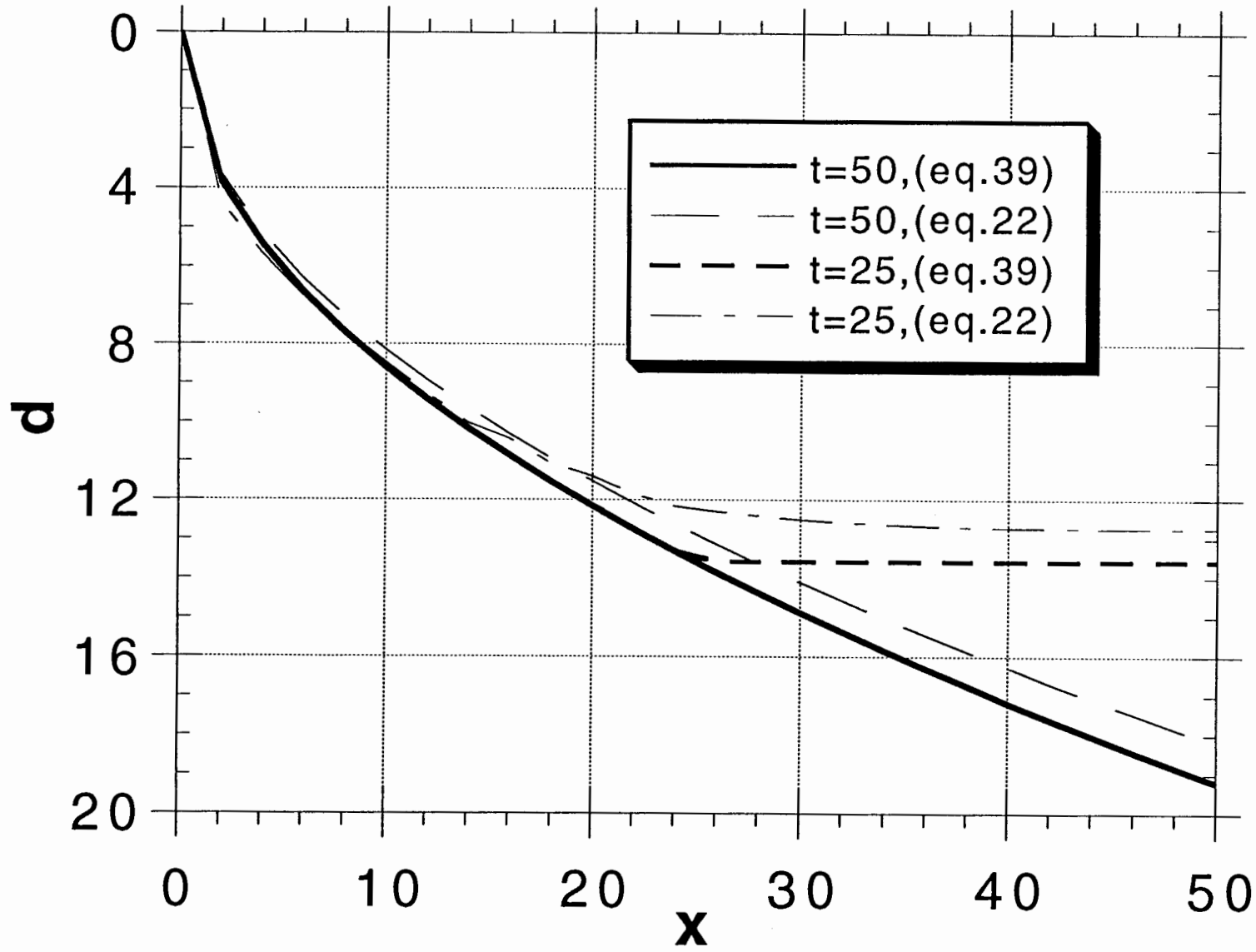

Fig. 13 Build-up of the contaminant concentration profiles in space and time as obtained by use of eq. (15) ($q_R = 0.1$, $a = 0.5$, $a_L = 5$).

(a) $t = 25$;

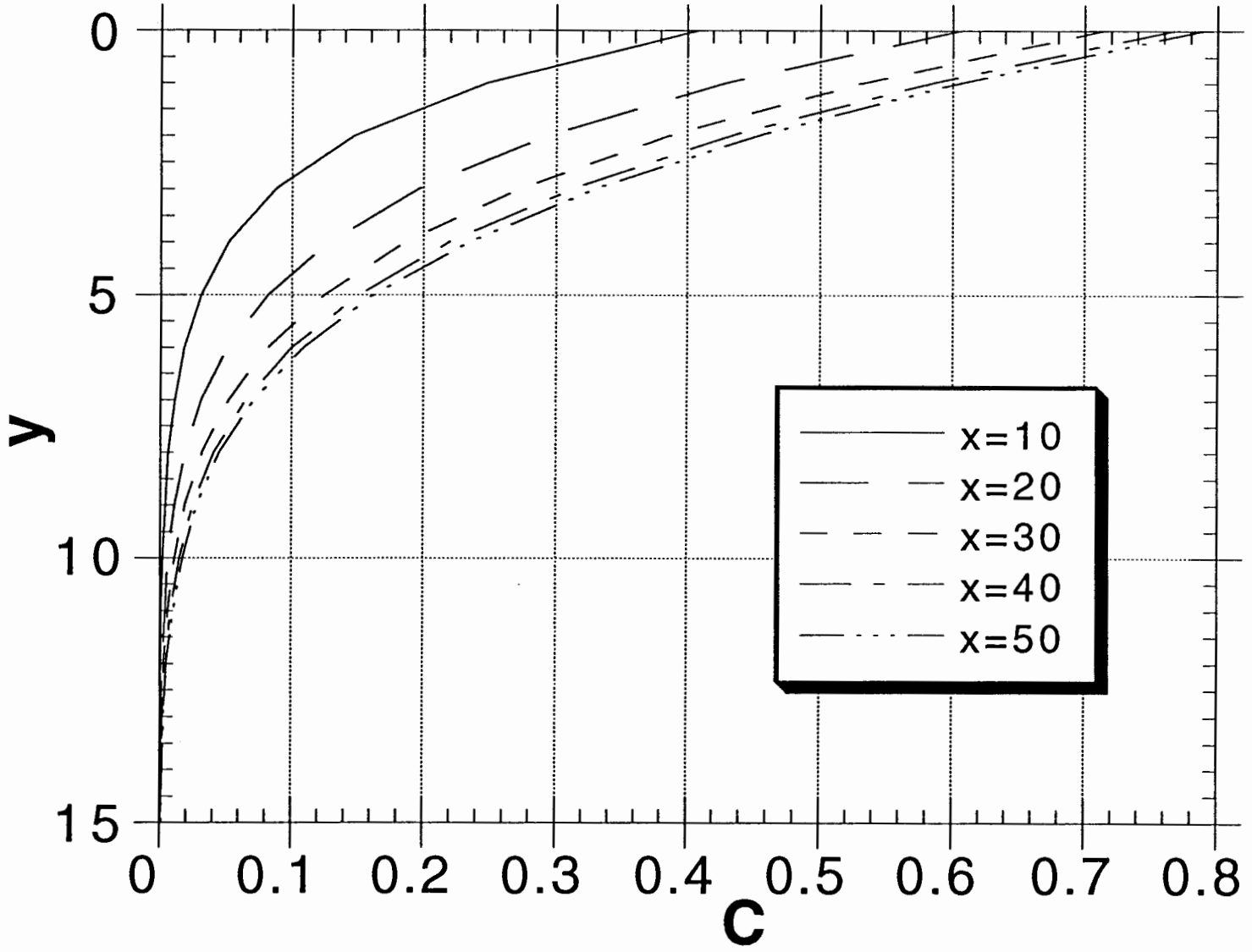

Fig. 13 Build-up of the contaminant concentration profiles in space and time as obtained by use of eq. (15) ($q_R = 0.1$, $a = 0.5$, $a_L = 5$).

(b) $t = 50$;

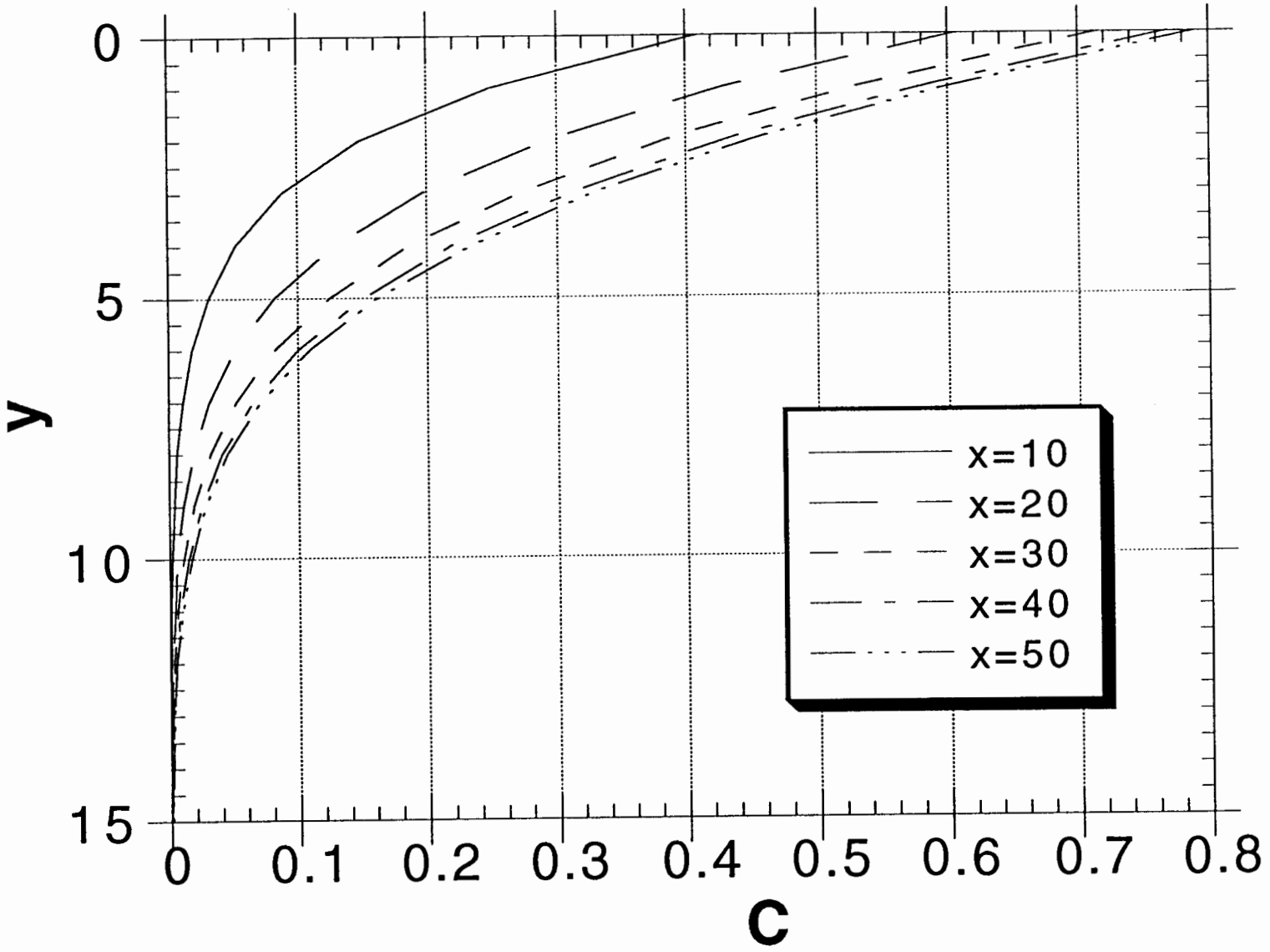

Fig. 13 Build-up of the contaminant concentration profiles in space and time as obtained by use of eq. (15) ($q_R = 0.1$, $a = 0.5$, $a_L = 5$).

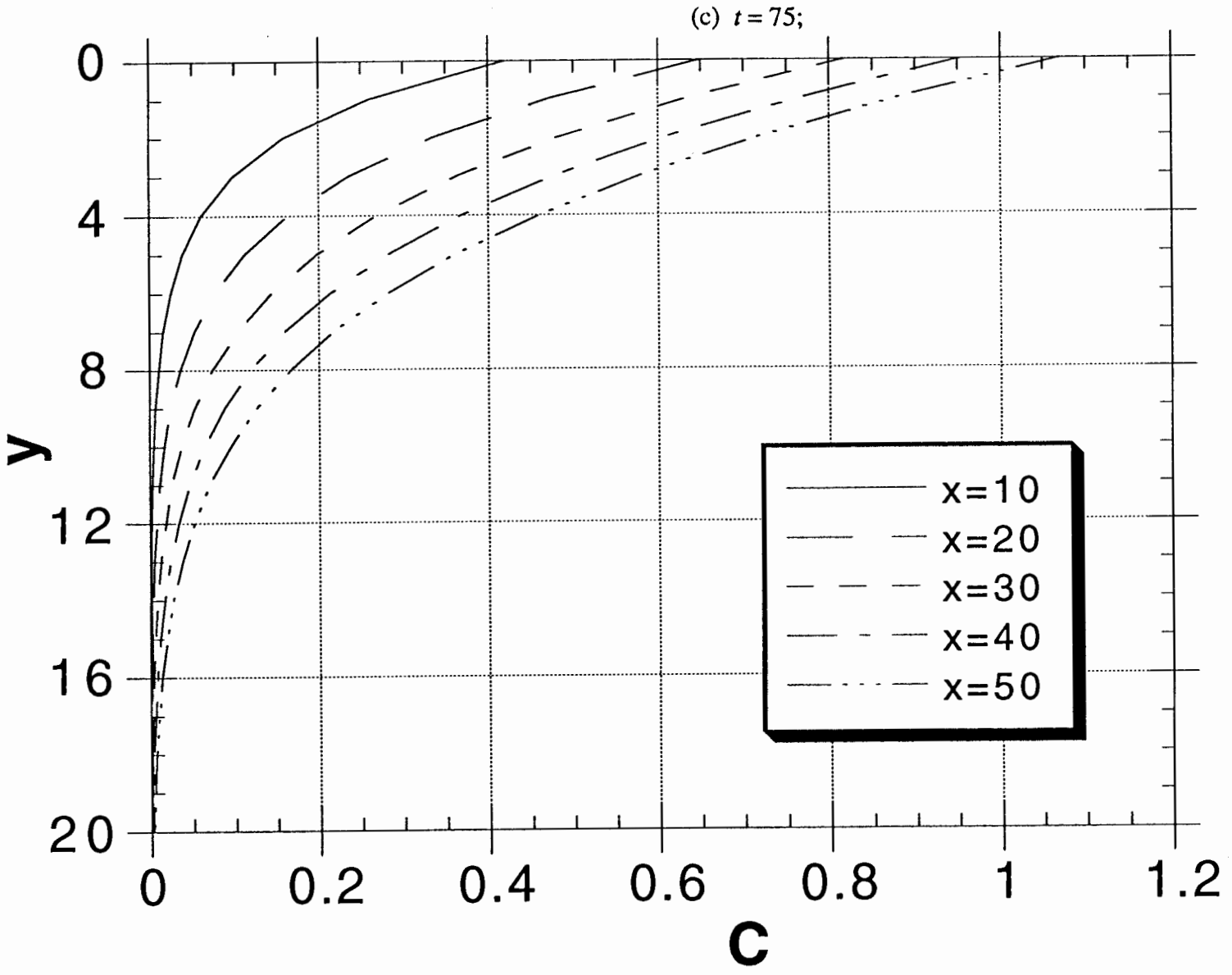

Fig. 13 Build-up of the contaminant concentration profiles in space and time as obtained by use of eq. (15) ($q_R = 0.1$, $a = 0.5$, $a_L = 5$).

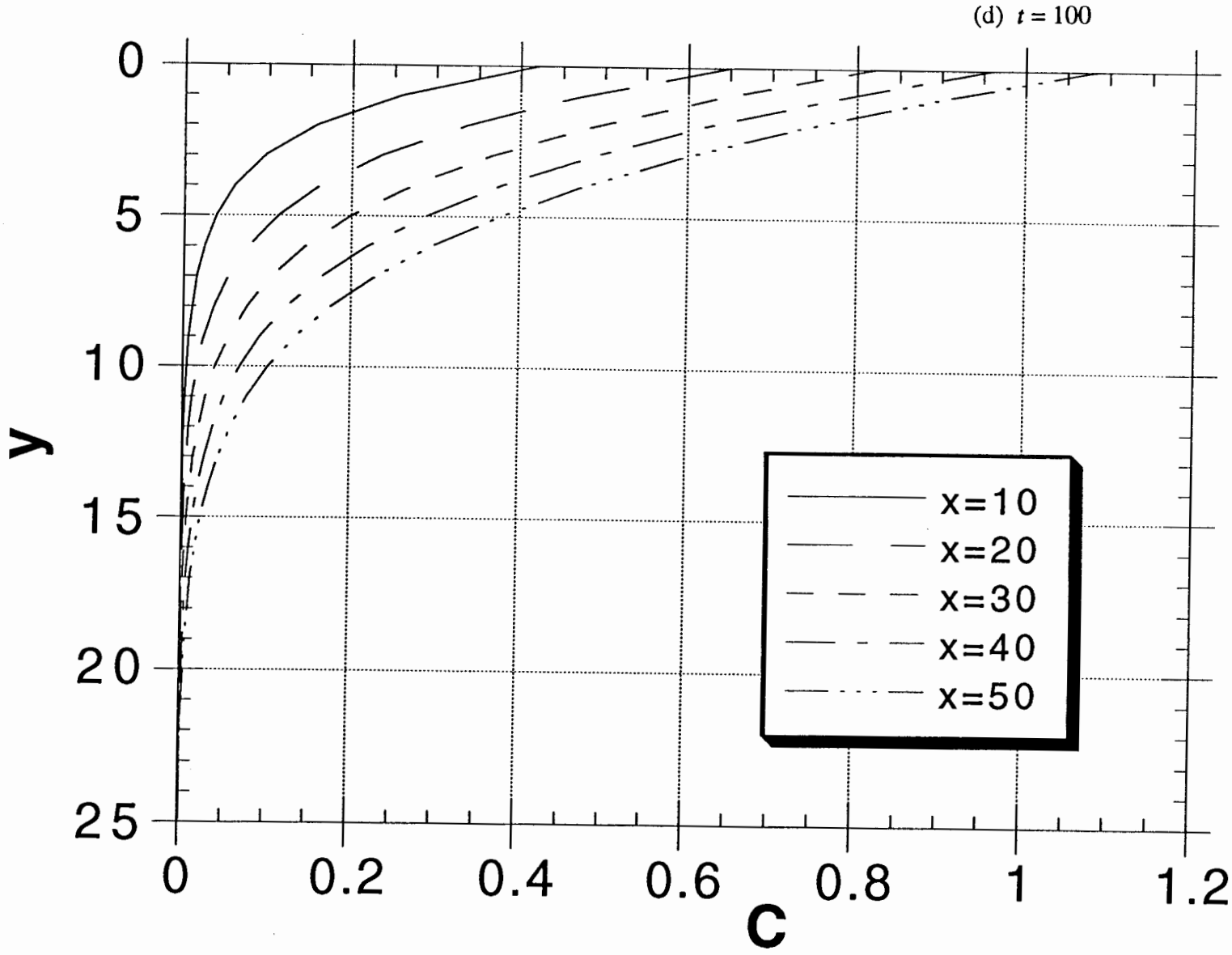

Fig 14 Build-up of the ROI in which $C \geq 0.01$, as obtained by use of eq. (15) ($q_R = 0.1$, $a = 0.5$, $a_L = 5$).

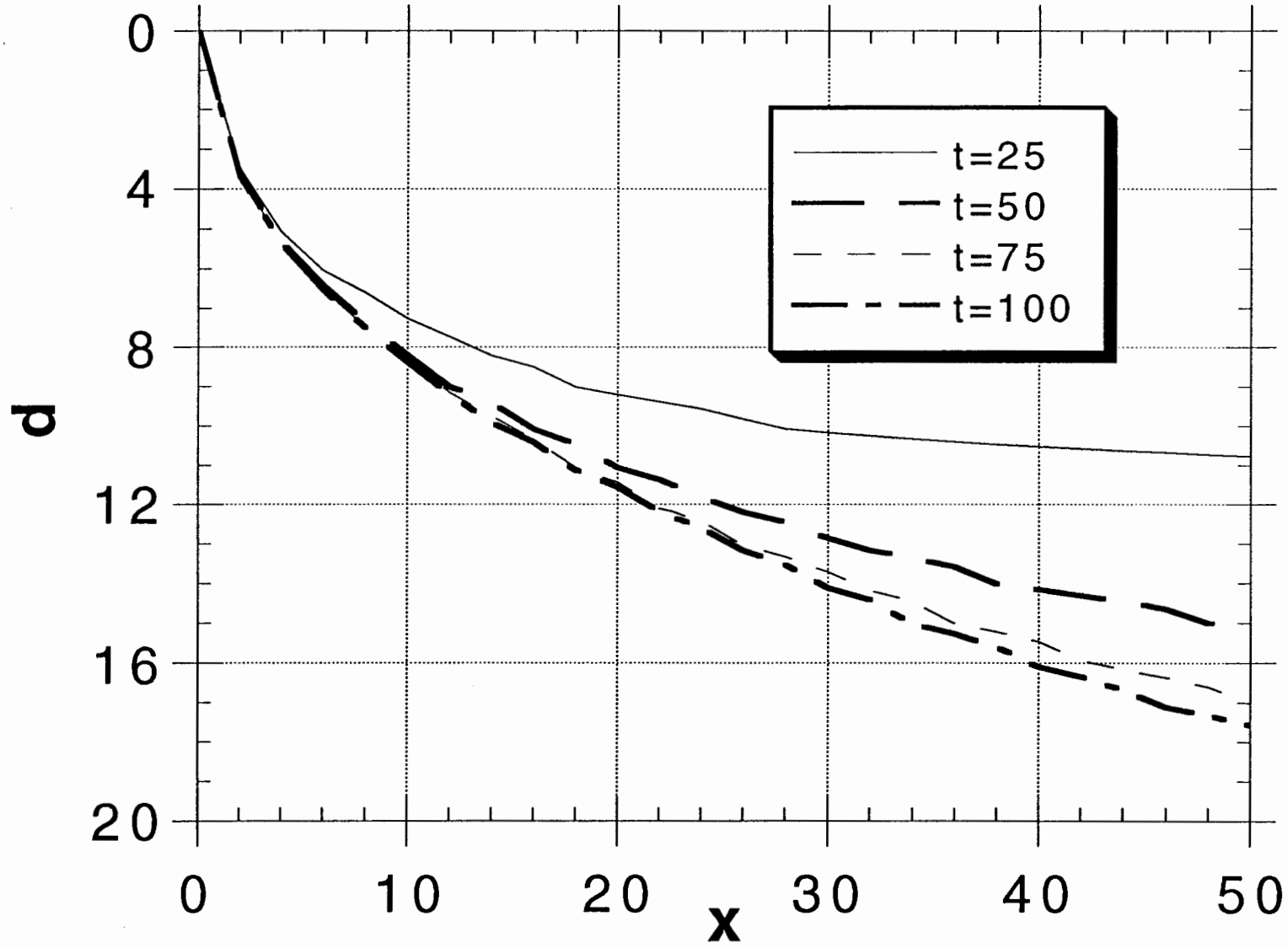

Fig. 15 Development of C_b in time and along the free surface of the aquifer according to eq. (15) ($q_R = 0.1$, $a = 0.5$, $a_L = 5$).

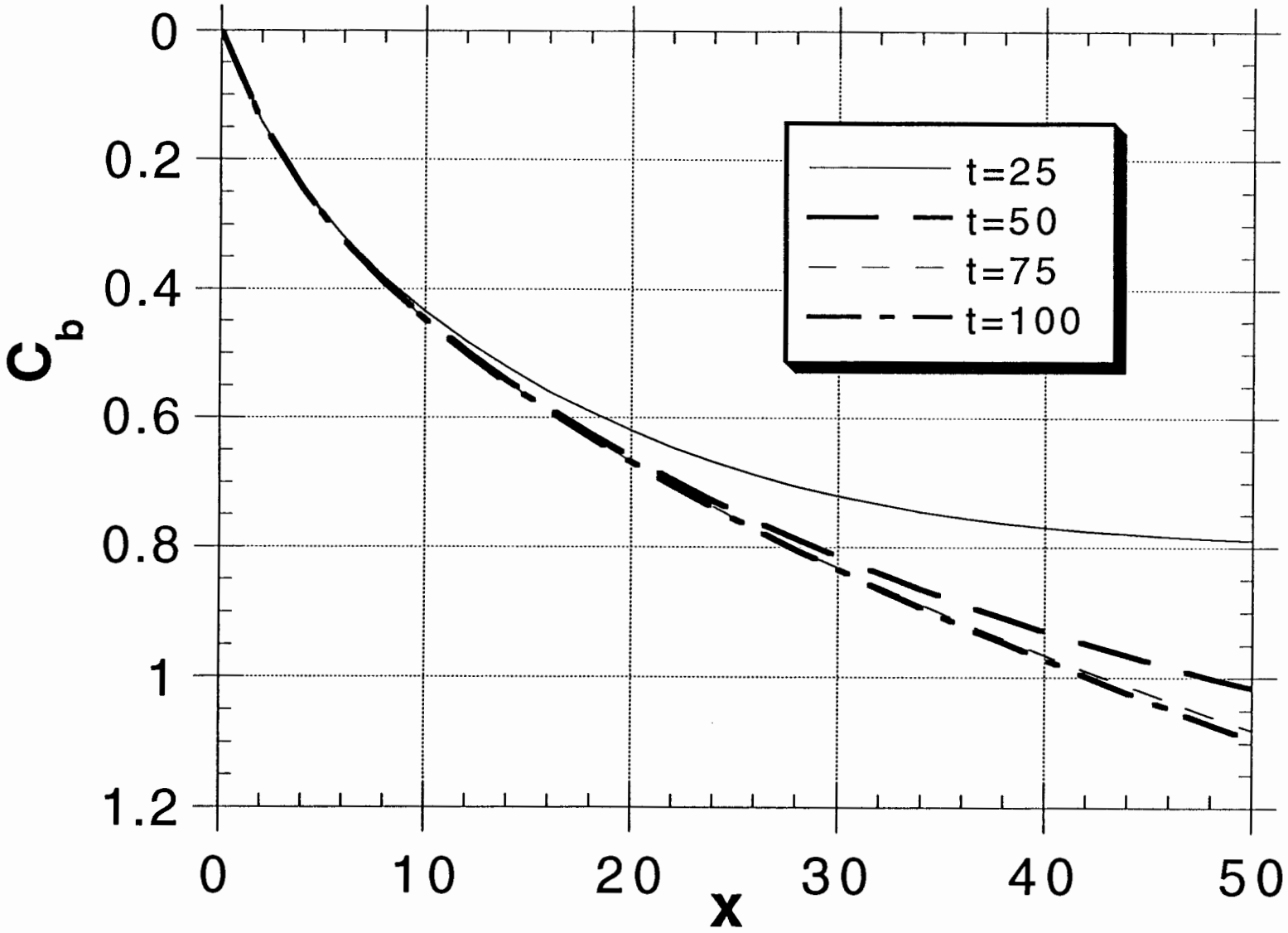

Fig. 16 Steady state profiles of C in various cross sections according to eq. (26) ($q_R = 0.1$, $a = 0.5$).

(a) $x = 10, 20, 30, 40, 50$

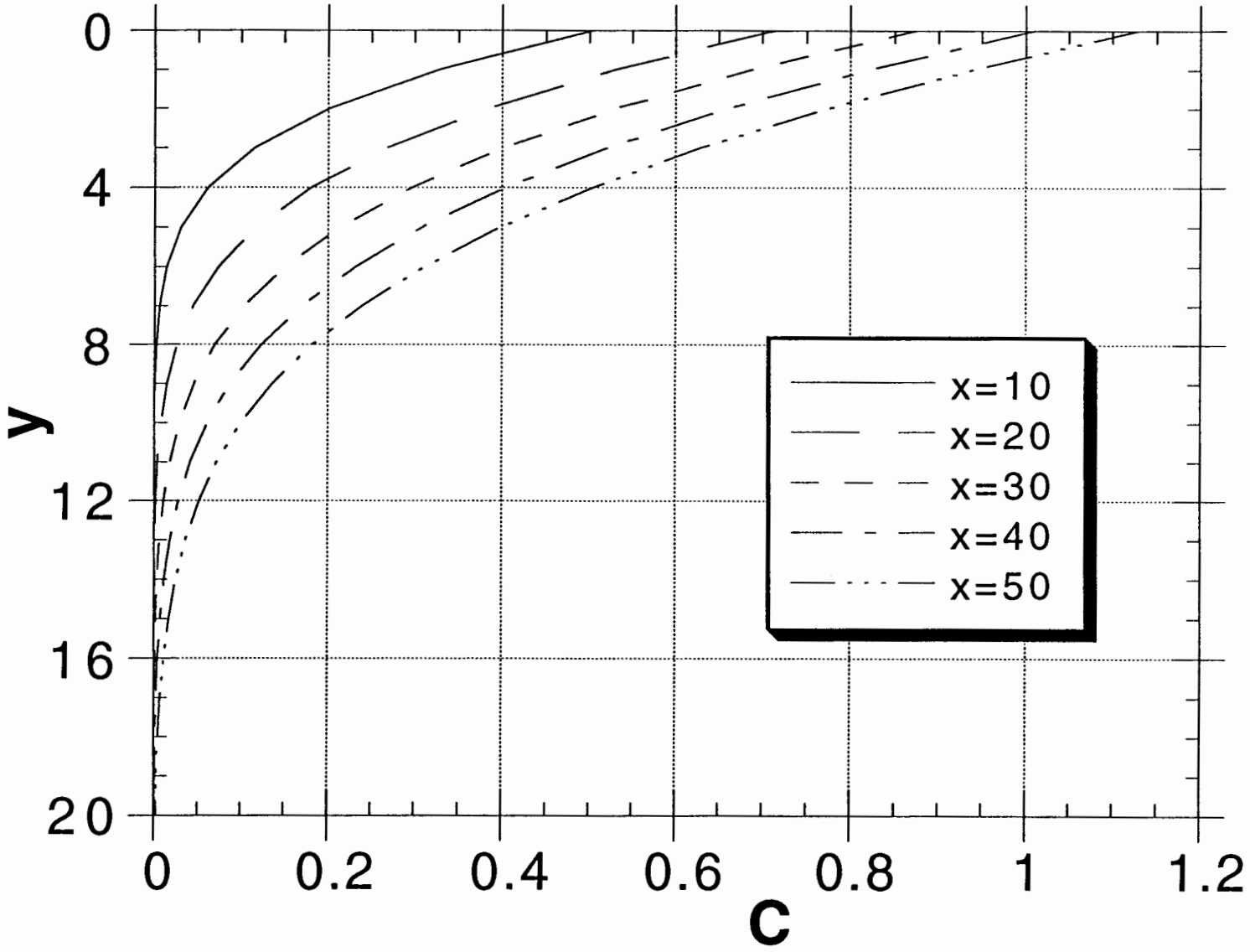

Fig. 16 Steady state profiles of C in various cross sections according to eq. (26) ($q_R = 0.1$, $a = 0.5$).

(b) comparison with eq. (19) ($a_L = 5$).

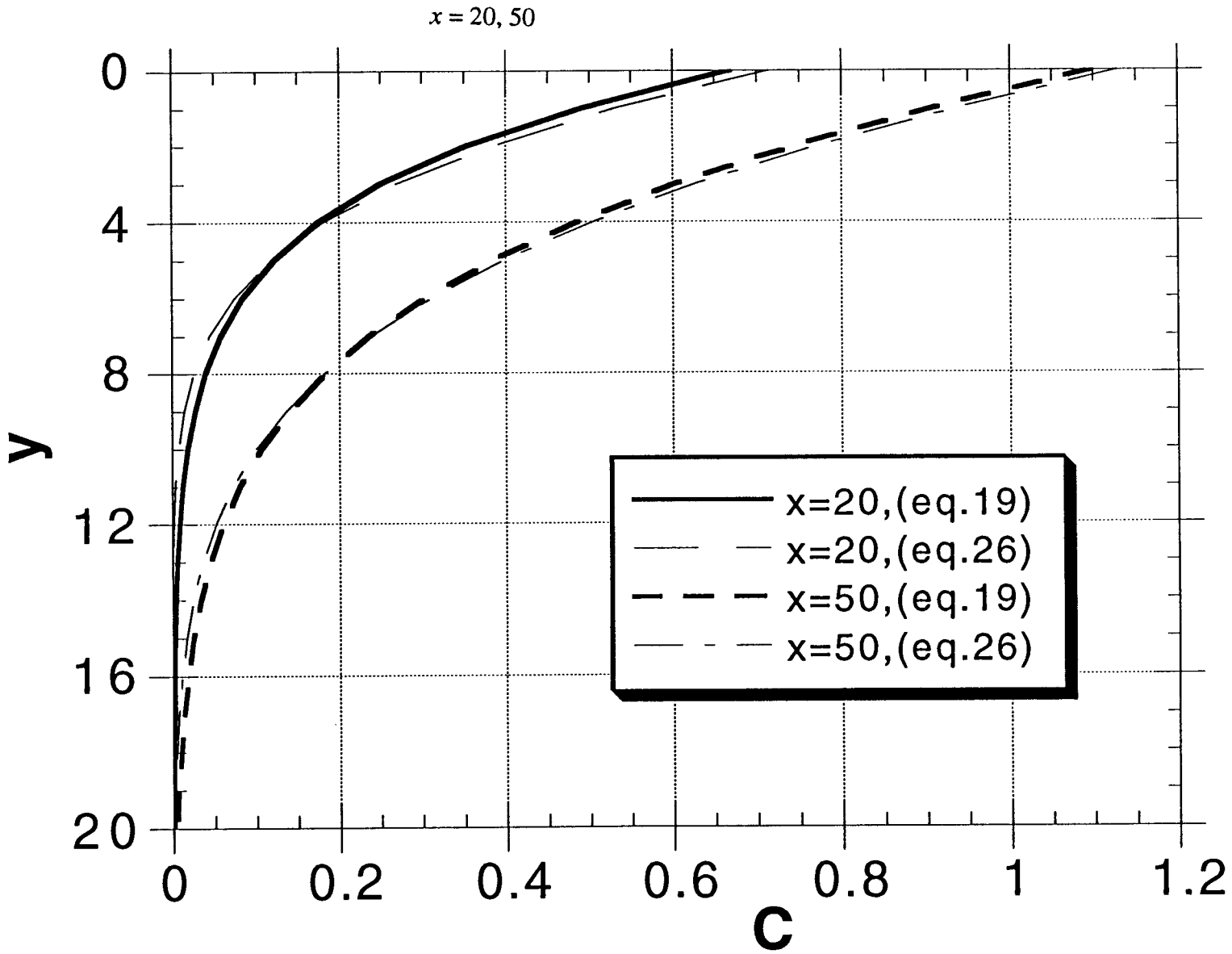

Fig. 17 Steady state C/C_b profiles versus y/δ_0 in various cross sections.

(a) $q_R = 0.001$; $a = 0.1$

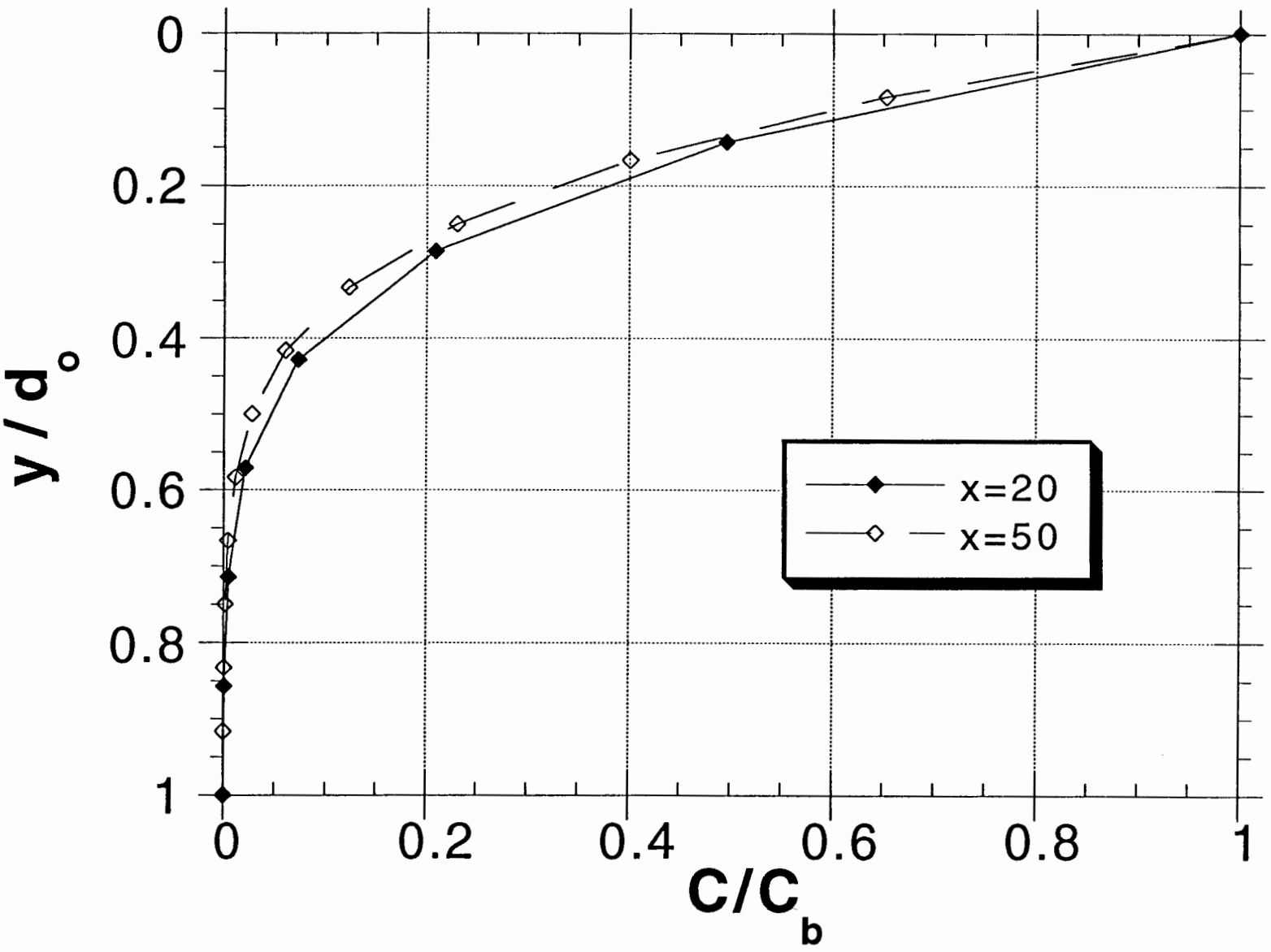

Fig. 17 Steady state C/C_b profiles versus y/δ_0 in various cross sections.

(c) $q_R = 0.01$; $a = 1$

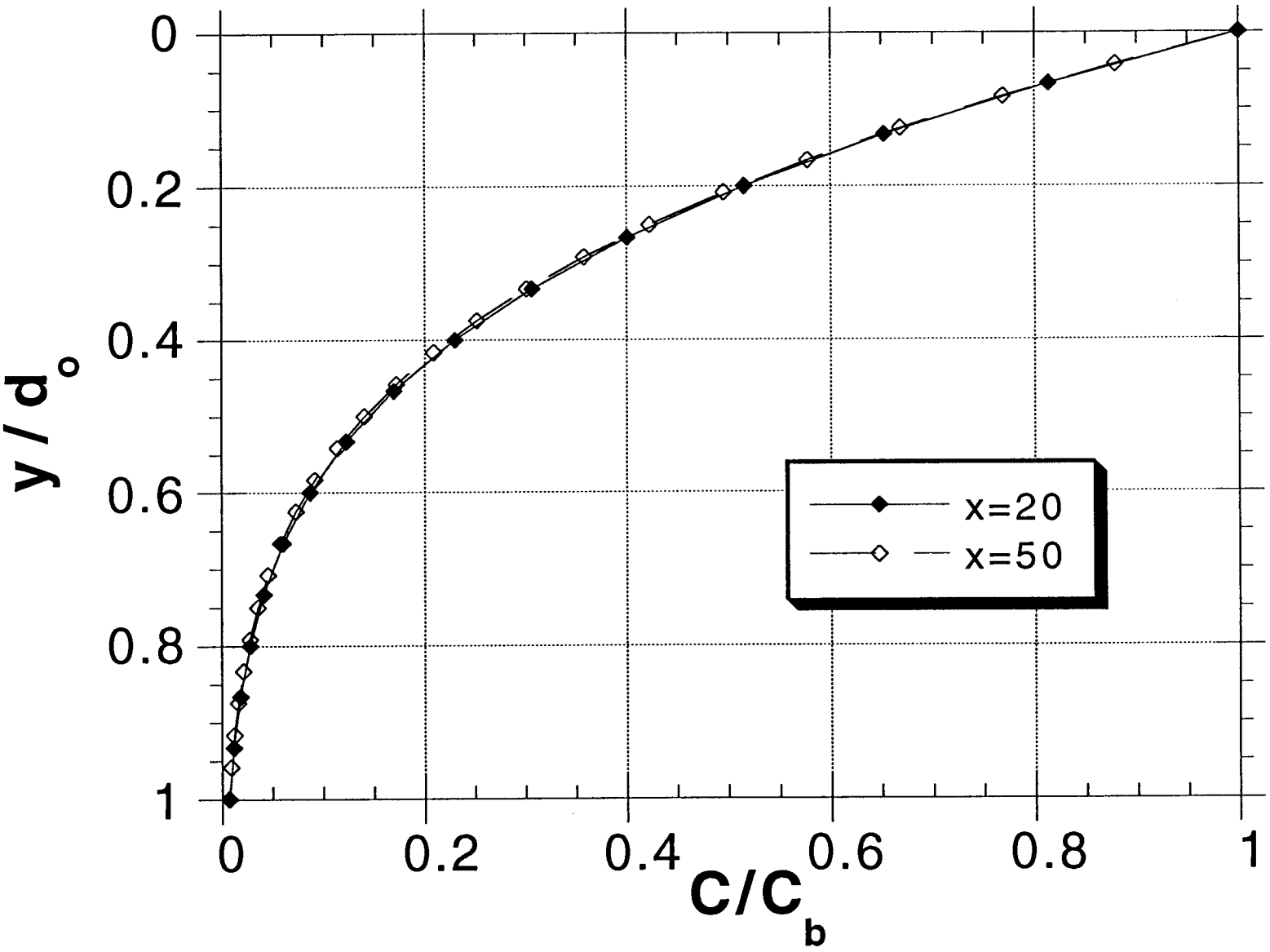

Fig. 17 Steady state C/C_b profiles versus y/δ_0 in various cross sections.

(b) $q_R = 0.01$; $a = 0.1$

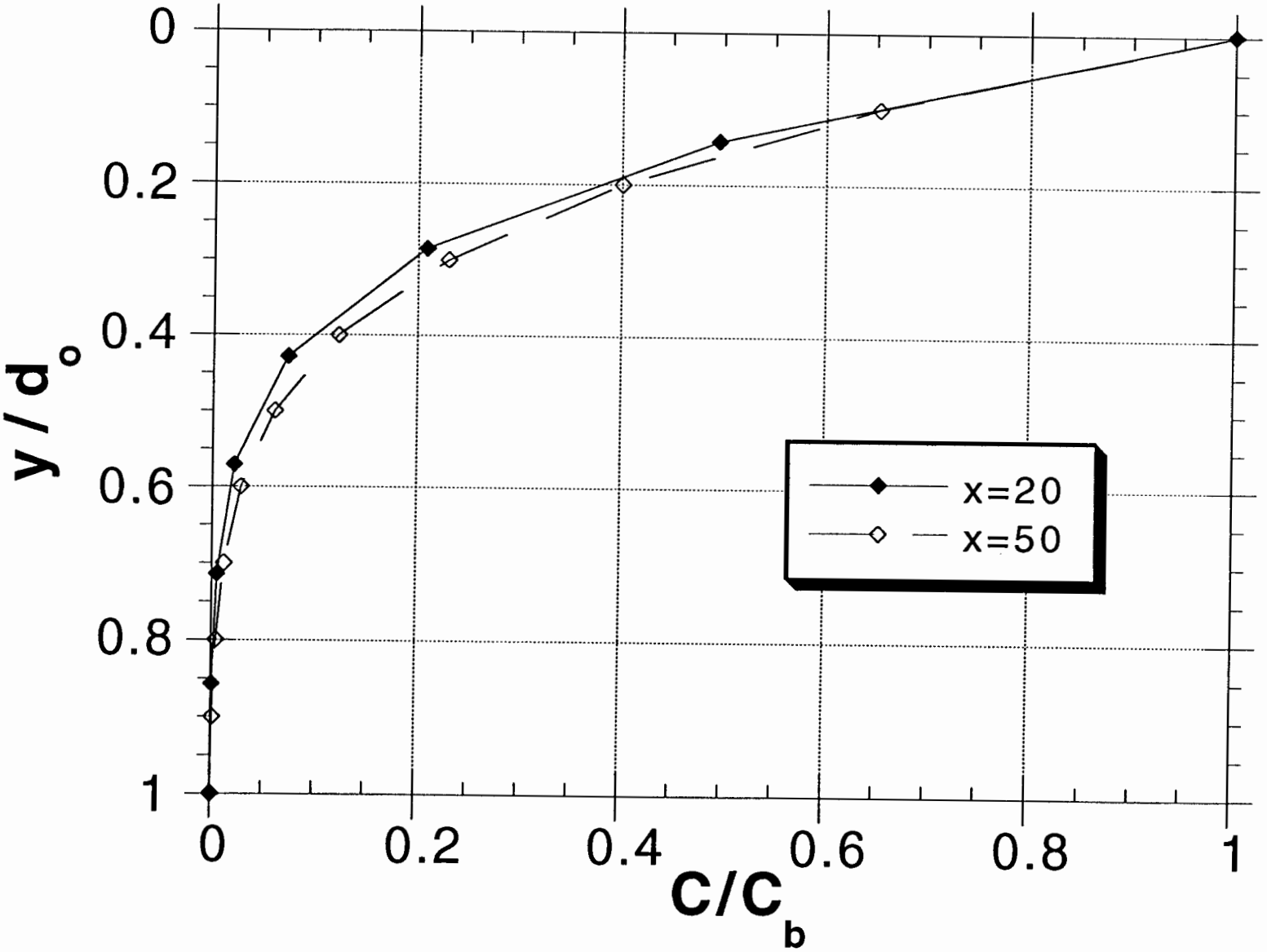

Fig. 17 Steady state C/C_b profiles versus y/δ_0 in various cross sections.

(d) $q_R = 0.1$; $a = 0.5$

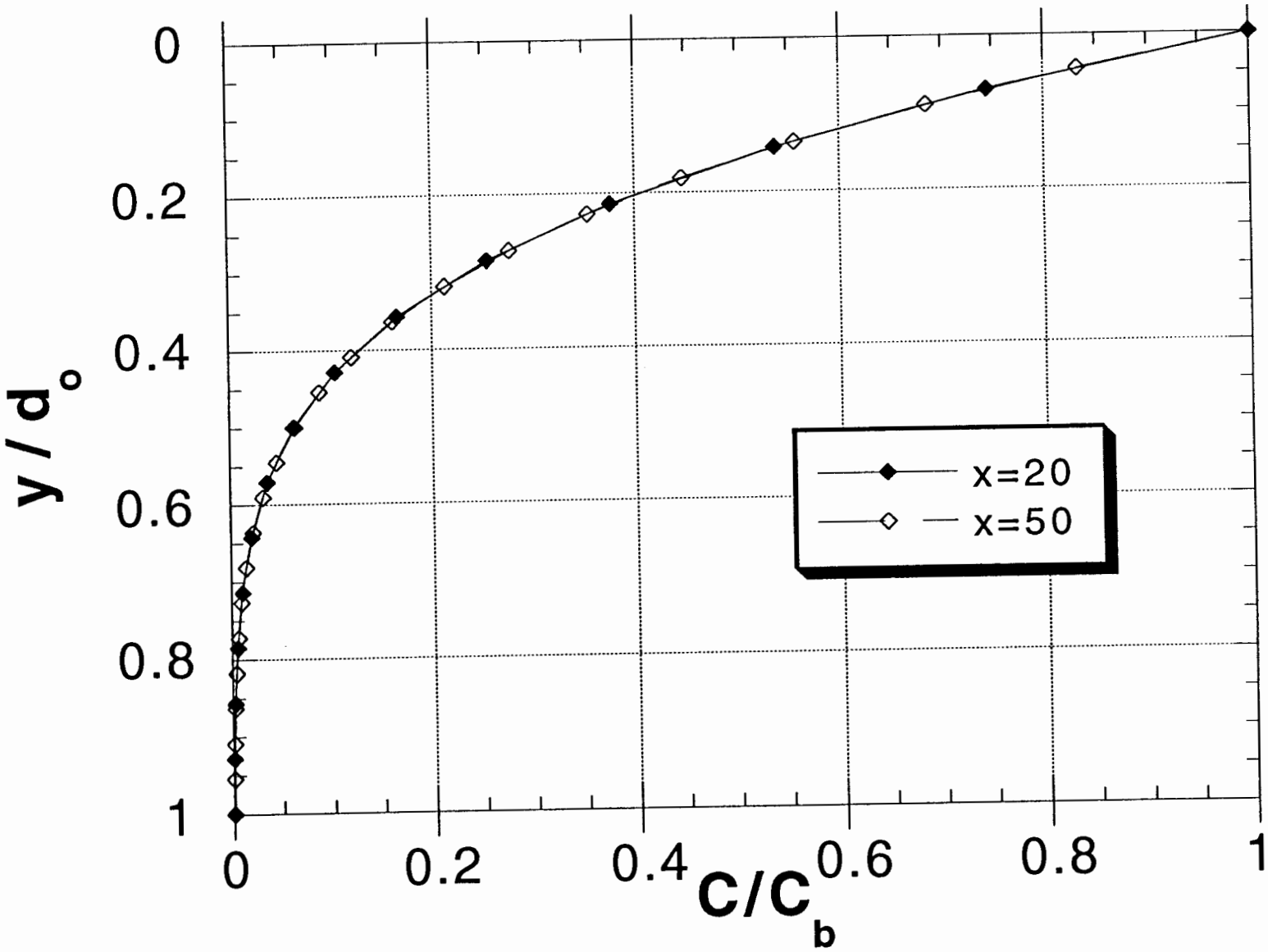

Fig. 18 Comparison between different power series expansions and C/C_b profiles at $x = 50$.

(a) $q_R = 0.001$; $a = 0.1$, $q_R/a = 0.01$

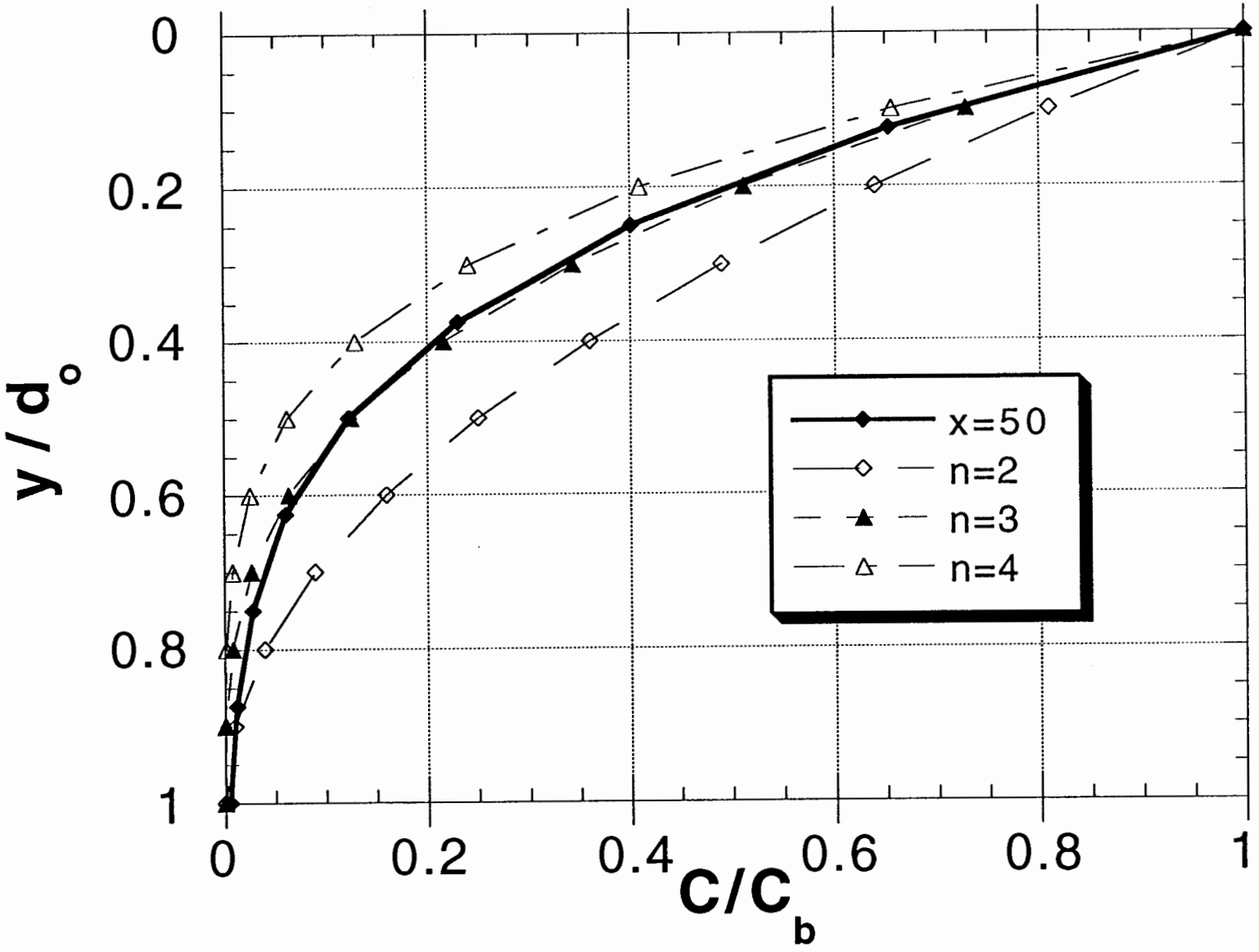

Fig. 18 Comparison between different power series expansions and C/C_b profiles at $x = 50$.

(b) $q_R = 0.01$; $a = 0.1$, $q_R/a = 0.1$

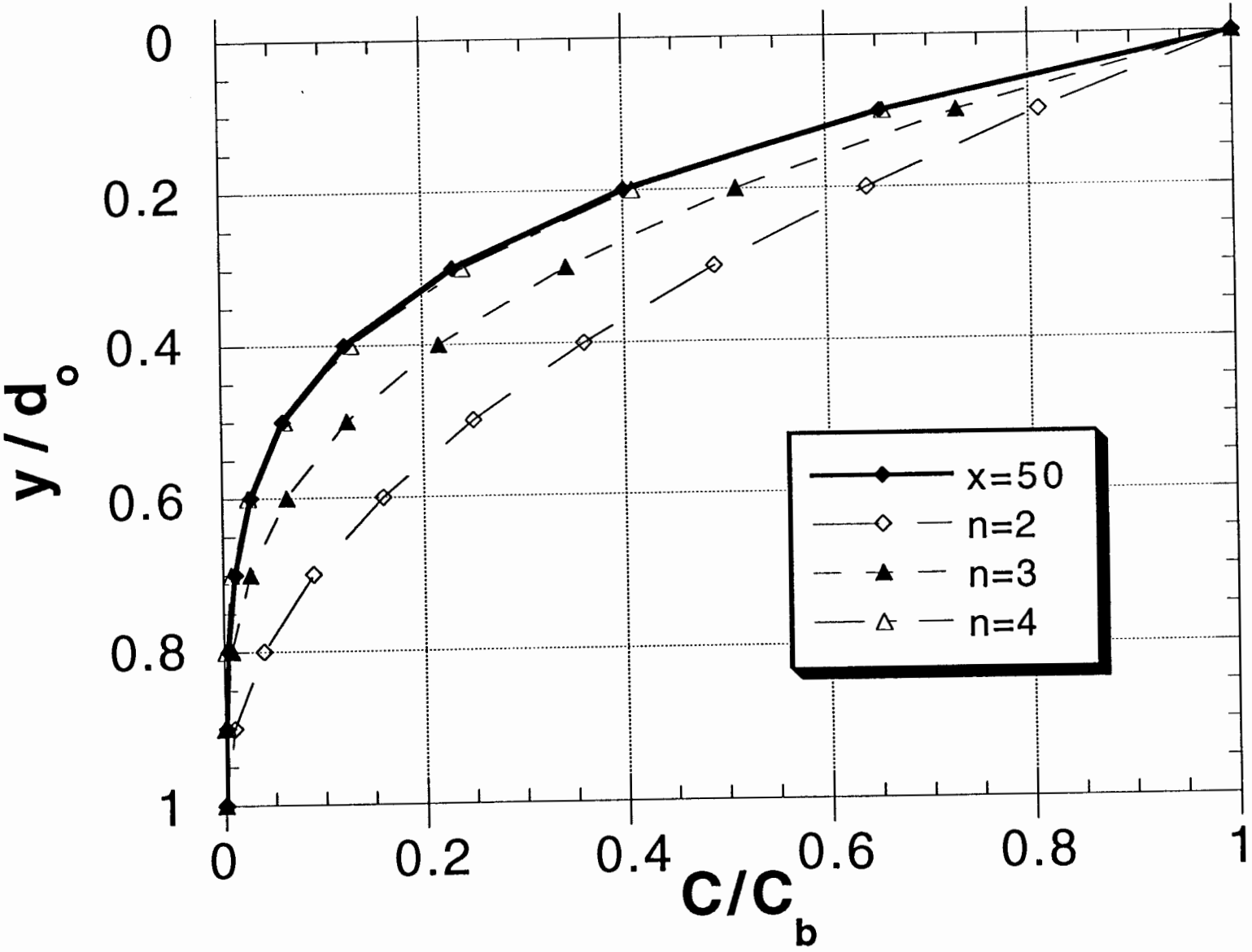

Fig. 18 Comparison between different power series expansions and C/C_b profiles at $x = 50$.

(c) $q_R = 0.01$; $a = 1$, $q_R/a = 0.01$

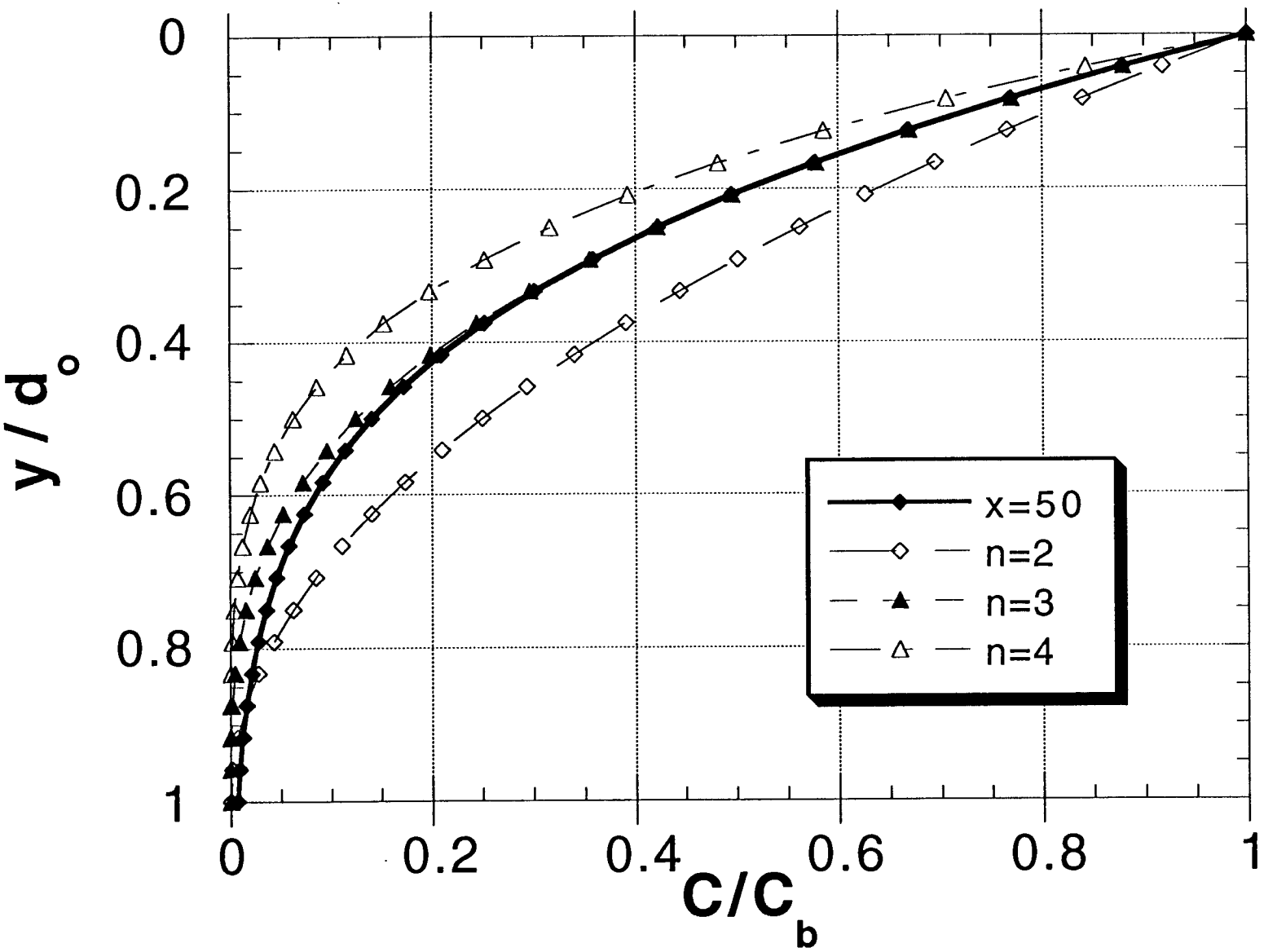

Fig. 18 Comparison between different power series expansions and C/C_b profiles at $x = 50$.

(d) $q_R = 0.1$; $a = 0.5$, $q_R/a = 0.2$

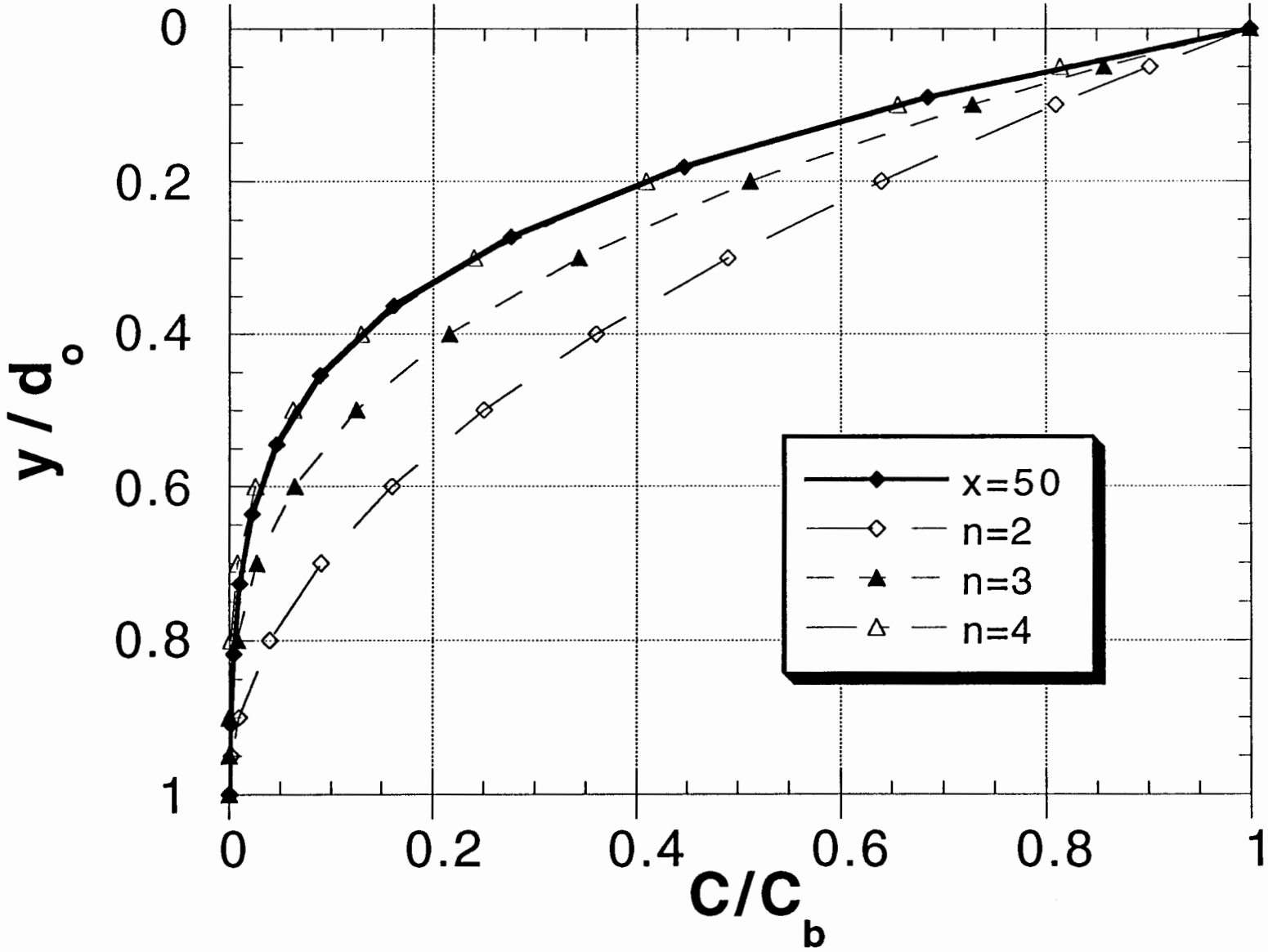

Fig. 19 Comparison between steady state values of δ and δ_0 obtained by TSBL approach and values of δ obtained by eq. (26).

(a) $q_R = 0.1$; $a = 0.5$, $n = 4$; $(q_R/a = 0.2)$

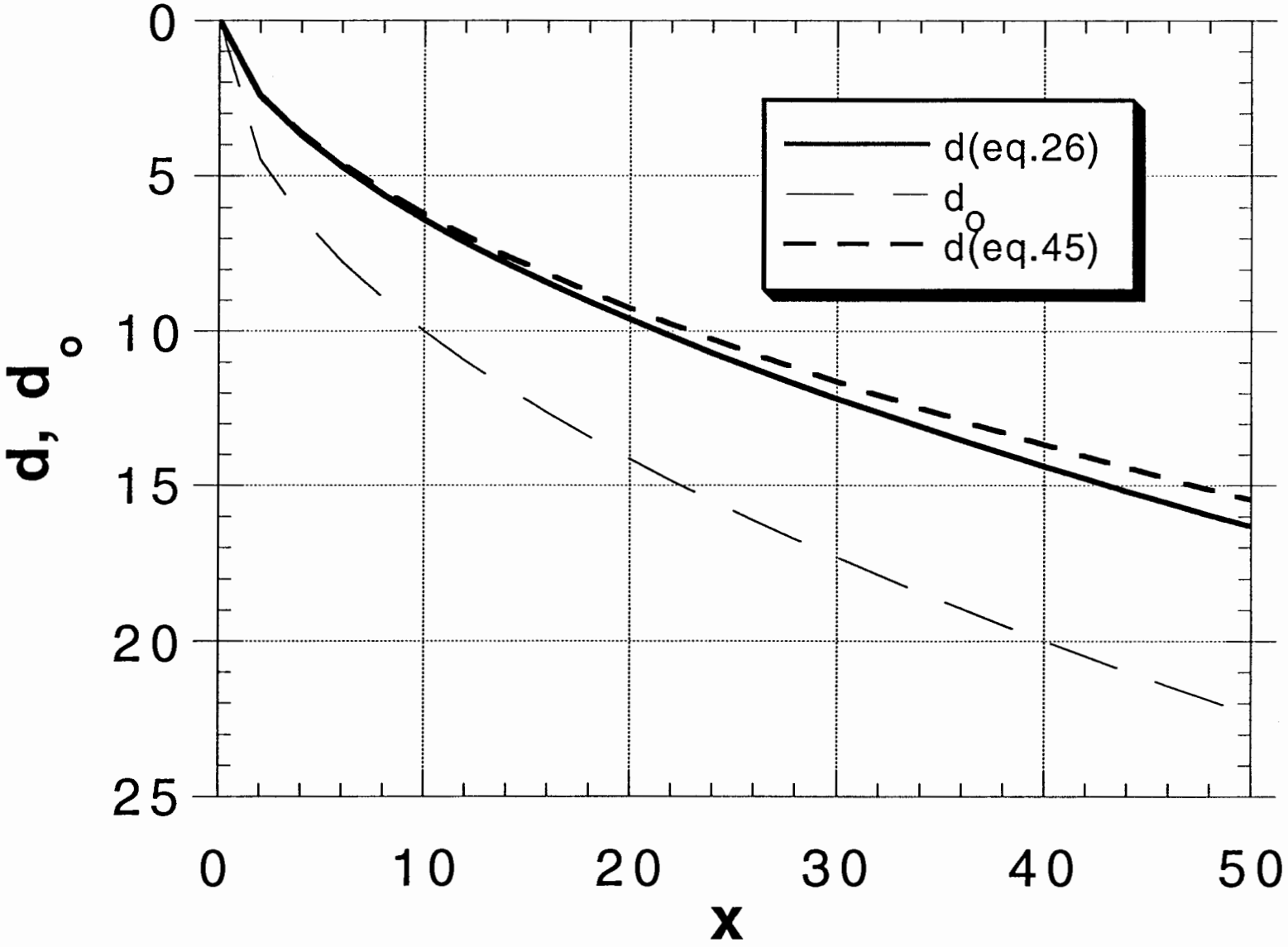

Fig. 19 Comparison between steady state values of δ and δ_0 obtained by TSBL approach and values of δ obtained by eq. (26).

(b) $q_R = 0.001$; $a = 0.1$, $n = 3$; $(q_R/a = 0.01)$

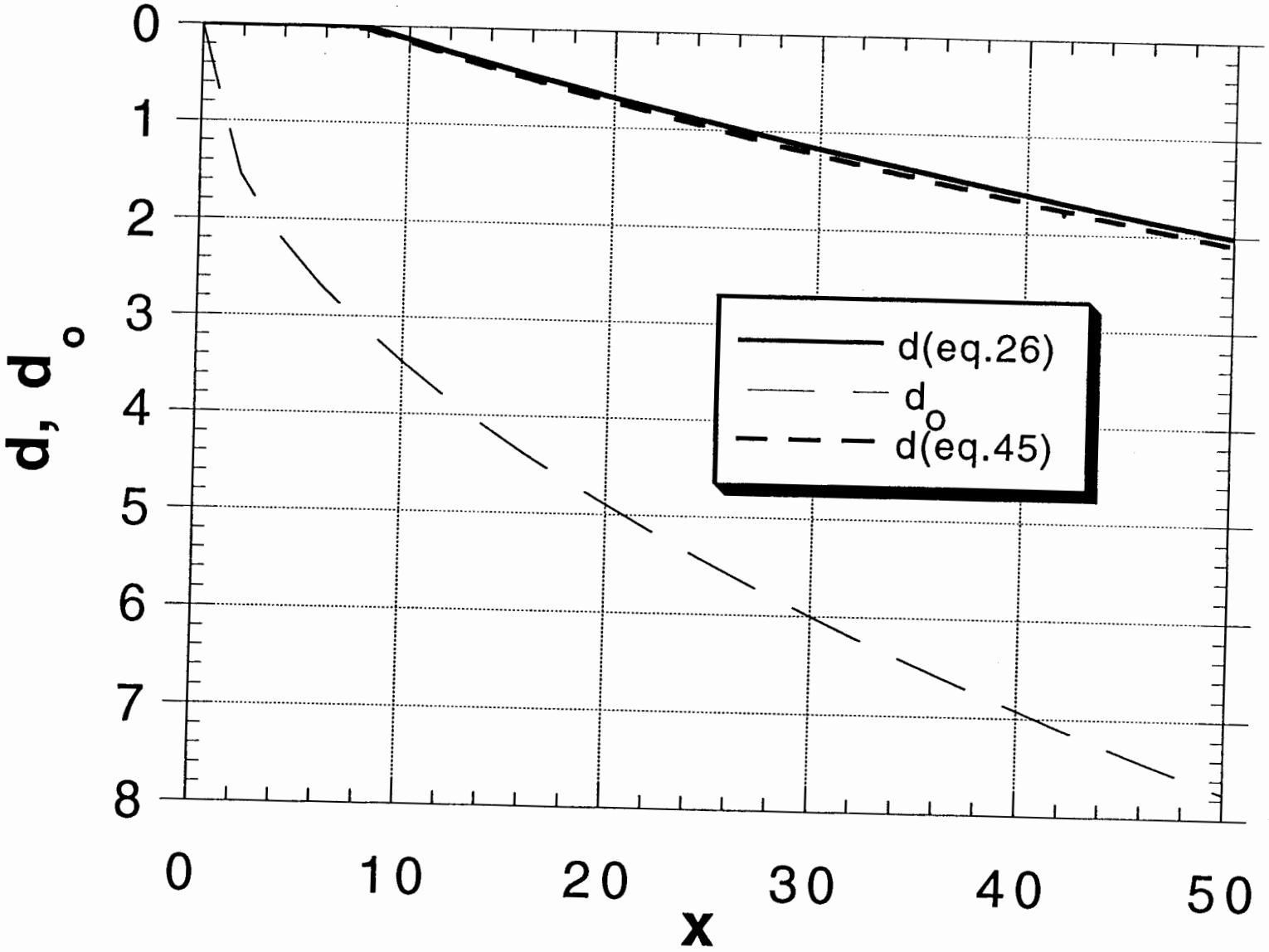

Fig. 20 Comparison between steady state values of C_b predicted by the TSBL method and values obtained by use of eq. (26).

Curves A—$q_R = 0.1$; $a = 0.5$, $n = 4$

Curves B—$q_R = 0.001$; $a = 0.1$, $n = 3$ (values are multiplied by 10)

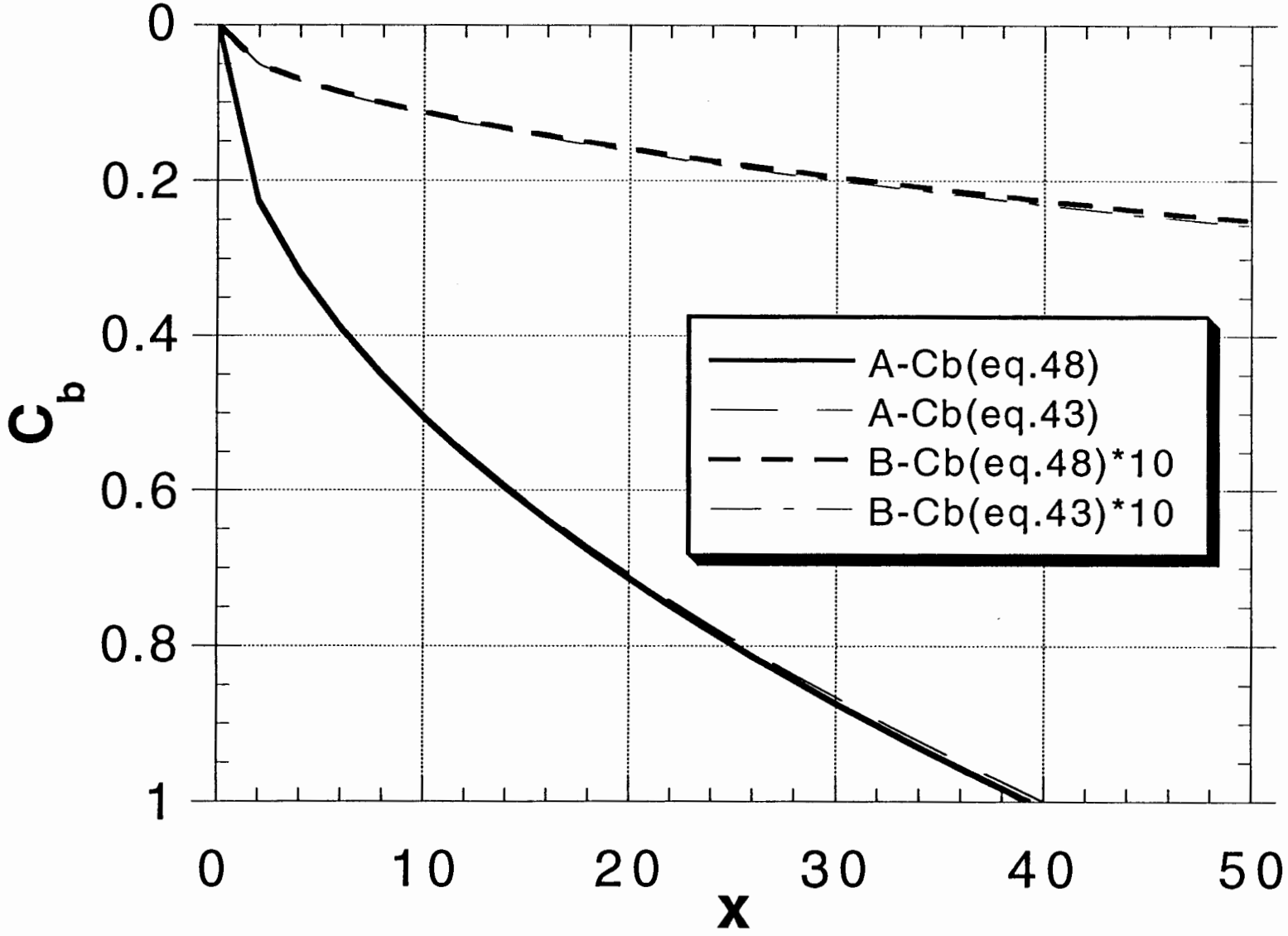

Fig. 21 Development of the ROI according to the TSBL method and the numerical scheme of eq. (22) ($q_R = 0.1$; $a = 0.5$, $n = 4$)